



Project Code: MQP JRB AL06

Research Techniques for Scald Burns

A Major Qualifying Project Report

Submitted to the University of

WORCESTER POLYTECHNIC INSTITUTE

In partial fulfillment of the requirements for the

Degree of Bachelor of Science

By:

Kathryn Hall

Sara Praschak

Carlos Vayas

Date: April 26, 2007

Approved: _____

Advisor, Professor Jonathan R. Barnett

TABLE OF CONTENTS

NOMENCLATURE	VI
EXECUTIVE SUMMARY	VII
ACKNOWLEDGEMENTS	X
1 INTRODUCTION	1
2 LITERATURE REVIEW	3
2.1 BURNS.....	3
2.1.1 <i>Skin</i>	3
2.1.2 <i>Burn Categories</i>	4
2.1.3 <i>Burn Experimentation</i>	6
2.1.3.1 <i>Henrique Burn Integral</i>	6
2.1.3.2 <i>Stoll and Chianta</i>	7
2.1.4 <i>Scald Burns</i>	9
2.2 FIRE PROTECTIVE CLOTHING	10
2.3 TESTING METHODS FOR FIRE FIGHTING CLOTHING	11
2.3.1 <i>Thermal Sensors</i>	12
2.3.1.1 <i>Copper Slugs</i>	12
2.3.1.2 <i>Epoxy-Glass Composite Sensors</i>	12
2.3.2 <i>Possible Large Scale Tests</i>	13
2.3.2.1 <i>Manikins</i>	13
2.3.2.1.1 <i>Thermo-Man®</i>	14
2.3.2.1.2 <i>ASTM F1930: Standard Test Method for Evaluation of Flame Resistant Clothing for Protection Against Flash Fire Stimulation Using an Instrumented Mannequin</i>	14
2.3.2.1.3 <i>Thermo-Leg®</i>	15
2.3.2.2 <i>Possible Small Scale Tests</i>	15
2.3.2.2.1 <i>Test for Thermal Protection Performance (TPP)/ ASTM D4108-87</i>	16
2.3.2.2.2 <i>Test for Radiant Protective Performance (RPP)/ ASTM F1939-99A</i>	17
2.3.2.2.3 <i>Cone Calorimeter Testing</i>	17
2.4 PAST MOISTURE STUDY	18
2.4.1 <i>Moisture Absorption in Turnout Garments</i>	18
2.4.2 <i>Moisture Transport in Turnouts</i>	19
2.4.3 <i>Developed Preconditioning Protocol</i>	20
2.4.4 <i>T-PACC Testing</i>	20
3 METHODOLOGY	22
3.1 POSSIBLE TEST METHODS	22
3.2 LABORATORY TESTING PROCEDURES OF MANIKIN	24
3.3 MATERIALS TESTING PROCEDURE	25
3.3.1 <i>Dry Materials</i>	25
3.3.2 <i>Wet Materials</i>	26
3.4 CONE CALORIMETER TESTING PROCEDURE	27
3.4.1 <i>First Tests: Glass-Epoxy Composite Sensors and Copper Slugs</i>	28
3.4.2 <i>Second Tests: Glass-Epoxy Composite Sensors at Low Heat Fluxes</i>	29
3.4.3 <i>Third Tests: Wet and Dry Cloth Samples for 390 Seconds</i>	30
3.4.4 <i>Fourth Tests: Wet and Dry Cloth Samples for 600/900 Seconds</i>	30
3.5 DEVELOPING GOVERNING EQUATIONS	31
3.5.1 <i>Heat transfer through moistened clothing</i>	31
4 RESULTS	36
4.1 CREATING A CURVE TO ANALYZE THE NEW SENSORS	36
4.2 FULL SCALE TESTING ANALYSIS.....	42
4.3 SMALL-SCALE TESTING – CONE CALORIMETER SERIES 1	48
4.4 SMALL-SCALE TESTING - CONE CALORIMETER SERIES 2.....	53
4.4.1 <i>Heat Flux and Burn Analysis</i>	53

5	CONCLUSIONS	63
6	RECOMMENDATIONS.....	66
	REFERENCES	67
	APPENDIX A	70
	<i>Outer Layer.....</i>	70
	<i>Moisture Barrier.....</i>	72
	Microporous Textiles	72
	Monolithic Textiles	72
	Bi-component Textiles.....	72
	<i>Thermal Liner</i>	73
	APPENDIX B.....	75

TABLE OF FIGURES

Figure 1: Layers of the Skin (AMA Atlas).....	4
Figure 2: Illustrations of First, Second, and Third Degree Burns.....	6
Figure 3: Stoll and Chianta Curve	8
Figure 4: Illustration of Thermo-Leg (R) Test.....	15
Figure 5: Layers of Thermal Barriers	16
Figure 6: Cone Calorimeter	17
Figure 7: Effect of Moisture Barrier Permeability and Thermal Liner and Sweat Accumulation in Firefighter Clothing in Wear.....	19
Figure 8: Setup for T-PACC Testing.....	21
Figure 9: Comparison of Wet and Dry Specimen using T-PACC.....	21
Figure 10: Thermocouple belt around the waist of manikin.....	25
Figure 11: Dressing manikin in large white cotton undershirt	26
Figure 12: Pour water into bucket.....	26
Figure 13: Half-immersed undershirt in water.....	27
Figure 14: Ring wet undershirt until there are no drips.....	27
Figure 15: Sensor inside fiberboard substrate with sample on top.	28
Figure 16: Assembly ready to be placed on stand	29
Figure 17: Illustration of Cone Calorimeter with Sample	31
Figure 18: Control Volume of the Moisture Barrier.....	32
Figure 19: Sensor Comparison Full Scale Test.....	36
Figure 20: Cone Test Results (5 kW/m ²).....	37
Figure 21: Cone Test Results (10kW/m ²).....	38
Figure 22: Cone Test Results (15 kW/m ²).....	38
Figure 23: Cone Test Results (20 kW/m ²).....	39
Figure 24: Cone Test Results (25 kW/m ²).....	39
Figure 25: New Curve Derivation Process	40
Figure 26: VHP Curve vs. Derived Curves	42
Figure 27: Wet versus Dry Test Averages.....	42
Figure 28: Full Scale Dry Temperature Averages.....	43
Figure 29: VHP vs. Dry Temperature Averages (14 sec).....	44
Figure 30: VHP vs. Dry Temperature Averages (10 sec).....	45
Figure 31: Full Scale Wet Temperature Results.....	46
Figure 32: VHP vs. Wet Temperature Averages (14 sec)	47
Figure 33: VHP vs. Wet Temperature Averages (10 sec)	47
Figure 34: Fabric Cone Test Epoxy-Glass Sensor.....	48
Figure 35: VHP vs. Fabric Cone Testing Epoxy-Glass Sensor	49
Figure 36: Fabric Cone Testing Epoxy-Glass Sensor.....	50
Figure 37: VHP vs. Fabric Cone Testing Epoxy-Glass Sensor	51
Figure 38: Fabric Cone Testing Copper Slug Sensor	52
Figure 39: Stoll and Chianta vs. Fabric Cone Testing Copper Slug Sensor	52
Figure 40: Stoll and Chianta vs. Projected Copper Slug Test.....	53
Figure 41: Heat Flux at Sensor - Dry Full Scale.....	54
Figure 42: Heat Flux at Sensor - Wet Full Scale	55
Figure 43: Time-Temperature Dry Full Scale	55

Figure 44: Time Temperature Dry Full Scale.....	56
Figure 45: Time Temperature, Dry (390 seconds).....	57
Figure 46: Time Temperature, Wet (390 seconds).....	58
Figure 47: Heat Flux at Sensor, Dry (390 seconds).....	58
Figure 48: Heat Flux at Sensor, Wet (390 seconds).....	59
Figure 49: Henrique's Burn Graph, Dry (390 seconds).....	59
Figure 50: Henrique's Burn Graph, Wet (390 seconds).....	60
Figure 51: Time Temperature, Dry (900 seconds).....	61
Figure 52: Heat Flux at Sensor, Dry (900 seconds).....	61
Figure 53: Henrique's Burn Graph, Dry (900 seconds).....	62

TABLE OF TABLES

Table 1: Stoll and Chianta Data Points	8
Table 2: Comparison of Different Large-Scale Test Methods.....	23
Table 3: Comparison of Different Small-Scale Test Methods.....	24
Table 4: Heat Fluxes Used in Second Tests.....	29
Table 5: New Curve Derived Points	41
Table 6: High Temp vs VHP Burns (Dry).....	45
Table 7: High Temp (Wet).....	48
Table 8: Globe Outer Shell Materials	70
Table 9: Comparison of Globe Moisture Barriers	73

Nomenclature

\dot{Q}_{rad}''	Radiation heat flux towards the skin (W/m ²)
\dot{Q}_{cond}''	Conduction heat flux towards the skin (W/m ²)
$\dot{Q}_{cond(skin)}''$	Conduction heat flux in the skin (W/m ²)
$\dot{Q}_{incident}''$	Incident heat flux towards the skin (W/m ²)
$\dot{Q}_{re-cond}''$	Re-conduction heat flux from the skin (W/m ²)
\dot{Q}_{re-rad}''	Re-radiation heat flux from the skin (W/m ²)
$\dot{Q}_{storage}$	Storage heat in the skin (J/K)
$\dot{Q}_{storage}''$	Storage heat flux in the skin (W/m ²)
\dot{m}_v''	Volumetric flow rate of vaporization (kg/m ³ s)
(Δh_v)	Latent heat of vaporization (J/kg)
k	Thermal Conductivity (W/m K)
T_f	Fabric Temperature-Cottons lower layer- (K)
T_s	Skin Temperature (K)
ε	Emissivity
σ	Stephan-Boltzmann Constant (W/m ² K ⁴)
m	Mass of skin layer to be studied (kg)
c_p	Specific heat of skin (J/kg K)
ℓ	Length of skin layer (m)
ρ	Density of skin (kg/m ³)

Executive Summary

Firefighters face many risks when doing their job; the most frequent injuries are burns. Burn injuries are costly to treat and, depending on the magnitude, greatly affect the livelihood of the firefighter. Firefighters are trained to be aware of these threats and manage their risks. But the danger of being burned and the loss of financial security is a constant worry for firefighters everyday (R. Lawson, 1998). From 2002 to 2007, there has been an average of 115 firefighter fatalities per year in the United States, from which an outstanding 4 - 5% are due to lethal burns. From this 4 – 5% of fatal burns, an average of one quarter are due to scald burns (Department of Homeland Security, 1999-2004 reports on Firefighter fatalities). Although scald burns are uncommon, they can cause debilitating injuries or even death.

Much research has been conducted in the field of skin burns, but because this research does not involve moisture, it does not directly correlate to scald burns. Stoll and Chianta developed a curve based on the heat flux generated at the surface of the skin and whether or not they could feel pain (Stoll and Chianta, 1971). The Henrique Burn Integral attempts to theorize the effect of high temperature on the skin. J.R. Lawson tested the thermal effect of firefighter protective clothing and has researched much about the skin when protected by clothing (Lawson, 1998). The effect of moisture beneath the protective clothing has been identified but little research has been performed.

To facilitate the progress, the goal of this project was to determine if scald burns could be tested in a lab setting to further facilitate future research with functional guidelines. In an attempt to accomplish this goal, a list of possible testing methods that could yield valuable information regarding scald burns was devised and a lab procedure for both test methods was created that would mimic a wet undergarment on a fire fighter. Wet and dry test results were compared to theoretical equations in order to examine the physical process of the test and the extent of the burns. Lastly, the different types of thermal sensors used in the project were compared to determine if the model derived by M.S Joel Sipe that does not account for the moisture barrier could be used in an

environment with a moisture barrier. With these objectives, it was found that it is possible to recreate scald burns in large-scale but not small-scale tests due to the lack of theoretical correlations which would take in account the effect of the moisture barrier.

To accomplish the first objective, a list of positives and negatives for each test was created. This list allowed us to identify which characteristics of the testing were important and to choose which test would fit the needs of this project. It was found that the test method suited for full-scale testing was to use a traversing manikin equipped with sensors and for the small-scale testing was the cone calorimeter.

To accomplish the second objective, the assumption was made that the amount of perspiration saturating the firefighter's undergarments is evenly distributed. This meant that the undergarment is completely saturated with water (no excess dripping and no dry areas). The developed lab procedure was found to be reproducible and had no visible error within each sampling. This same procedure was used for large- and small-scale testing. To better understand the collected data, we needed to understand the phenomenon occurring at the sensor.

To accomplish the third objective, theoretical equations for a scald burn were investigated. This allowed us to compare the wet testing with a model that might explain what is happening. When the wet and dry tests were compared, the wet tests indicated that the skin was actually cooling instead of receiving a burn faster than when the skin was dry. An explanation for this might include the following. Since the sample was soaked with water, the pores of the fabric were filled and as a result, a moisture barrier was created. The water in the pores absorbed the energy from the fire which vaporized the water, never allowing the energy to reach the skin.

To accomplish the last objective, two data interpreting methods were used. One method applied to specific type of copper slugs we were provided and the other to the epoxy-glass composite sensors. The data for the copper slugs was analyzed using a previous method from Joel Sipe's WPI M.S. Thesis. This allowed us to convert the

collected data into time-temperature data, heat flux data, and burn data. The burn data plotted the times and temperatures at which first- and second-degree burns occurred. The epoxy-glass composite data was analyzed using a method based off from the Stoll and Chianta curve. Time versus change in temperature data was plotted with the Stoll and Chianta curve. A separate curve at each heat flux was generated, allowing us to find where burns occurred on the manikin in large-scale testing. The comparison between both of these data interpreting methods showed us that a discrepancy exists between when a moisture barrier is and is not present. Temperatures of around 200°C were recorded at the skin level when using M.S Joel Sipe's model but there was no trace of a second-degree scald burn in the analysis. This is quite incongruent since second-degree burns appear at temperatures of about 55°C.

With these objectives, it was found that it is possible to reproduce scald burns in large-scale tests but not small-scale tests due to the lack of theoretical correlations which would take into account the effect of the moisture barrier. Further research should be conducted to get more accurate models.

A model to quantify the quality of the input received by the epoxy-glass composite sensors should be developed. The current data from the report suggest that due to manufacturing procedures and due to the lack of information on these composite sensors, their output data can be highly unreliable. Therefore, using copper slugs would produce readable and accurate results. The group also believes that the data collected with the epoxy-glass composite sensors has a significant degree of deviation from reality due to the above-mentioned concern.

Acknowledgements

Joel Sipe, PhD candidate mentored us throughout this project making sure we understood the burn process completely. He also gave us any other advice we asked for and was a great moral support for this entire project.

Randy Harris taught us how to run tests on the cone calorimeter. He found time for us in his busy testing schedule to help us and to fix the sensors that we broke.

Dr. Ned Keltner provided us with information about the epoxy-glass composite sensors when we were at wit's end. He is a great source of information and willing to help.

Dr. Roger Parry of E. I. du Pont de Nemours and Company provided us with advice about using the epoxy-glass composite sensors without overstepping any legal ties.

Dr. J.R. Lawson of the National Institute of Standards and Technology answered all of our questions promptly and in depth that pertained to moisture in firefighters suits. For that, we are grateful.

Lelia Lawson helped us track down her thesis in hopes of expanding her research through this project.

Andrew Ellison and the Navy Clothing and Textiles Research Facility provided us with the test facilities, the epoxy-glass composite sensors, and the materials to carry out this project.

Again, thank you to all who helped us complete this project.

1 Introduction

Firefighters face many risks when doing their job, including burns which are the most frequent injury. Burn injuries are costly to treat and, depending on the magnitude, greatly affect the livelihood of the firefighter. Firefighters are trained to be aware of these threats and manage their risks, but the danger of being burned and the loss of financial security is a constant worry for firefighters (R. Lawson, 1998). From 2002 to 2007, there has been an average of 115 firefighter fatalities per year in the United States, from which an outstanding 4 - 5% are due to lethal burns. From this 4 – 5% of fatal burns, an average of one quarter is due to scald burns (Department of Homeland Security, 1999-2004 reports on Firefighter fatalities). Although scald burns are uncommon, they can cause debilitating injuries or even death.

Researchers may not have focused their efforts on scald burns because of the few statistics that can be found on them. Many incidents with scald burns do not get reported because they can be cured by applying ice to the site (Firefighter Gilbert A. Lefort, personal communication regarding scald burns, April 2, 2007). Therefore, a lack of development has hindered great advances in this research field.

Much research has been conducted in the field of skin burns, but because this research does not involve moisture, it does not directly correlate to scald burns. Stoll and Chianta developed a curve based on the heat flux generated at the surface of the skin and whether or not they could feel pain (Stoll and Chianta, 1971). The Henrique Burn Integral attempts to theorize the effect of high temperature on the skin. J.R. Lawson tested the thermal effect of firefighter protective clothing and has researched much about the skin when protected by clothing (Lawson, 1998). The effect of moisture beneath the protective clothing has been identified as a factor in scald burns but little research has been performed.

The absence of research in this area provides the opportunity to examine laboratory testing procedures for scald burns. This project brings attention to this

recurring concern in firefighter's lives. Furthermore, such research may provide the foundation for protective fire gear, such as materials that do not allow moisture beneath firefighter protective clothing.

To facilitate the progress, the goal of this project was to determine if scald burns could be tested in a lab setting to further facilitate future research with functional guidelines. In an attempt to accomplish this goal, a list of possible testing methods that could yield valuable information regarding scald burns was devised and a lab procedure for both test methods was created that would mimic a wet undergarment on a fire fighter. Wet and dry test results were compared to theoretical equations in order to examine the physical process of the test and the extent of the burns. Lastly, the different types of thermal sensors used in the project were compared to determine if the model derived by M.S Joel Sipe that does not account for the moisture barrier could be used in an environment with a moisture barrier. With these objectives, it was found that it is possible to recreate scald burns in large-scale but not small-scale tests due to the lack of theoretical correlations which would take in account the effect of the moisture barrier.

2 Literature Review

2.1 Burns

To better understand how burns occur, the structure and functions of the skin should be understood. This chapter will also present how scald burns occur on the skin. Lastly, the thermal characteristics of the human skin and how researchers have related them to mathematics will be discussed.

2.1.1 Skin

The human skin is the largest organ in the body (BBC, 2005). The skin represents approximately 15% of the total weight of an adult and has a surface area of approximately 1.7 m² (Beyler...[et al], 2000). The skin performs numerous tasks that are essential for living. Among the most important ones:

- Protection of underlying tissues from physical or thermal trauma
- Thermal regulation of the body by sweating and heat conduction
- Impermeability to tissue fluids
- Sensory Perception of touch pain and temperature

As with the multiple tasks it performs, its physiology is equally complex. It is because of this reason that models and algorithms only provide an estimate of skin damage and not a clear-cut result.

The skin is composed of three primary layers: the epidermis, the dermis and hypodermis. The outer layer is the thinnest and it is referred to as the epidermis. The basal layer, not shown in Figure 1, appears at the bottom of the epidermis and is approximately 80 µm below the surface (Sipe, 2004). The basal layer is considered a thin transitional layer between the epidermis and the dermis and is not a primary layer. The next layer is called the dermis and is a thicker layer and usually referenced as an outer layer. Below the dermis is the subcutaneous tissue or hypodermis (Beyler...[et al], 2000). Within these layers of skin are nerves that serve to relate the surrounding world to the

brain. Stimulus such as cold, hot, pain, pressure and touch are all transmitted through the nerves located in your skin (AMA Atlas).

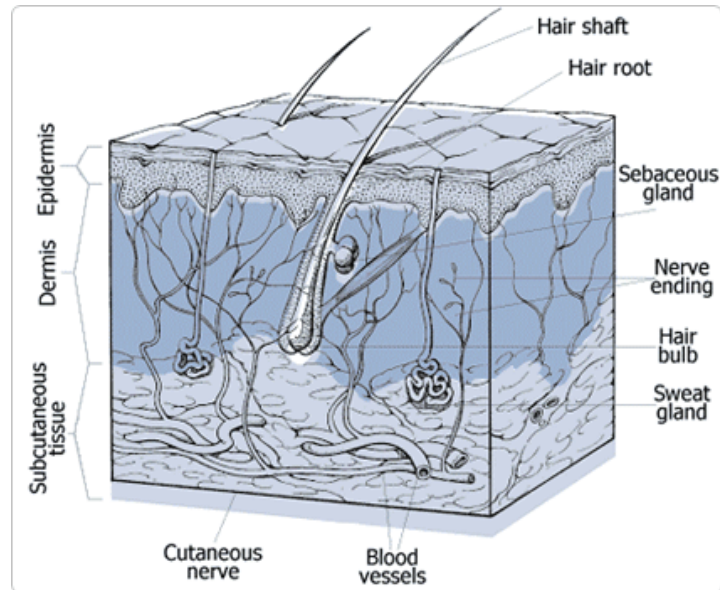


Figure 1: Layers of the Skin (AMA Atlas)

Skin acts as the primary protection for the body, protecting from UV radiation, temperature extremes, bacteria, and toxins (Revis, 2006). Severe burns can affect the skins' ability to protect the body as well as cause irreversible damage.

2.1.2 Burn Categories

There are four different types of burns, thermal burns, chemical burns, electrical burns, and radiation burns (Children's Hospital of Philadelphia, 2006). This project deals primarily with thermal burns specifically scald burns.

Over the years many different schemes to evaluate a thermal injury have been developed. The most common method is to rank burns as first-, second-, or third- degree burns which depends strictly on the level of necrosis and depth of damage caused to the skin (Beyler...[et al], 2000). Other methods include classifying the burns as partial or full thickness burns or by the change of pigmentation in the epidermis.

First-degree burns are categorized as superficial burns where only the epidermis is affected. The skin is typically red and painful and does not blister and its related magnitude is that of severe sunburn (Ahrenholtz...[et al.], 1995). First-degree burns occur when the basal layer reaches approximately 48°C and usually cause pain, redness, and minor swelling (Lawson, 1996).

A second-degree burn is indicative of complete necrosis of the epidermis while visually it can be detected by the presence of blisters (Beyler...[et al], 2000). If no damage occurs to the dermis then it is considered a superficial second-degree burn. If minor damage to the dermis occurs it is considered a deep second-degree burn. (Ahrenholtz...[et al.], 1995). A second-degree burn occurs at approximately 55°C and affects the sweat glands and the hair follicles (Lawson, 1996).

A third-degree burn is indicative of complete necrosis of the dermis, possibly extending to the hypodermis (Beyler...[et al], 2000). With a third-degree burn the skin rarely blisters, it is dry, gray and charred. (Ahrenholtz...[et al.], 1995). Usually there is no feeling and no possibility for skin regeneration.

Additional levels of burns exist within this scheme but they are rarely mentioned due to their lack of occurrence. Fourth-degree burns require a skin graft, fifth- and sixth-degree burns involve destruction of the muscle and the bone, respectively (Purser, 1996).

Scald burns can cause anywhere from first to third degree burns (Burn Survivors throughout the World). Figure 2 shows the extent of first-, second-, and third- degree burn damage.

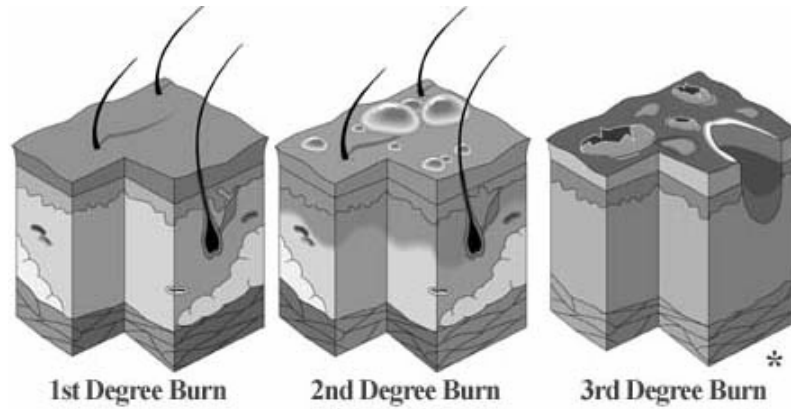


Figure 2: Illustrations of First, Second, and Third Degree Burns

2.1.3 Burn Experimentation

Over 500,000 treatments were received for burn injuries in America in 2006 (American Burn Association, 2006). These drastic numbers indicate that scientific experimentation to determine how and at what temperatures burns occur should be investigated. Two methods of experimentation that identify second- and third- degree burns are discussed below.

2.1.3.1 Henrique Burn Integral

The Henrique Burn Integral estimates the time it takes to receive a second or third degree burn. The equation for the Henrique Burn Integral is shown in Equation 1.

$$\frac{d\Omega}{dt} = P \exp\left(\frac{-\Delta E}{RT}\right) \quad (1)$$

In the Henrique Burn Integral, seen in Equation 1, where “ Ω is the measure of burn damage, P is a human skin system constant, T is temperature, t is time, R is the universal gas constant and ΔE is the activation energy of human skin” (Barker, Guerth-Schacher, et al., p.30). The value of ΔE is 6.28E8 J/kmol and the value of P is 3.1E98 1/s (Sipe, p.10). Integrating Equation 1 in terms of Ω is shown in Equation 2.

$$\Omega = \int_0^t P \exp\frac{\Delta E}{RT} dt \quad (2)$$

For $\Omega < 0.5$, there is no damage at the basal layer (the deepest layer of the epidermis); for $0.5 < \Omega < 1$, first degree burns develop; $\Omega = 0.53$ is the point where a first degree burn starts (Cavanagh, p.14). For $\Omega > 1$, second and third degree burns occur. Using the Henrique Burn Integral, data may be inputted to determine the duration of time it will take for a certain degree burn to occur from an elevated temperature setting.

2.1.3.2 Stoll and Chianta

Stoll and Chianta have conducted extensive research about predicting when burns occur. Their work started in the 1960's, and their research was based upon quantifying the response of human skin and tissue to sources of heat energy (Stoll and Chianta, 1968, 1969).

Stoll and Chianta discovered that if the normal blood temperature of human tissue is raised from its normal, 36.5°C, to 44°C, skin burns will begin to occur. As an example, burns occur nearly one hundred times faster at 50°C than at 44°C; which shows that skin burns are related to length of exposure as well as temperature (Stoll and Chianta, 1971). Also, at 72°C the epidermis is destroyed almost immediately (Stoll and Chianta, 1971). These examples illustrate that the “rate at which damage to the skin occurs will increase logarithmically with a linear increase in temperature” (Sipe, 2004).

These experiments were carried out with the use of calorimeter sensors, more specifically, copper disks with known heat capacity and with thermocouples attached to the bottom which recorded the data. Table 1 correlates the data shown in Figure 3, which is a typical output of a sensor reading of this kind, better known as the Stoll and Chianta curve.

Exposure Time (s)	Heat Flux (cal/cm ² sec)	Heat Flux (kW/m ²)	Calorimeter Equivalent Temperature Rise (°C)
1	1.2	50.0	8.9
2	0.93	38.8	10.8
3	0.55	22.9	12.2
4	0.45	18.8	13.3
5	0.38	15.8	14.1
6	0.34	14.2	15.1
7	0.3	12.5	15.5
8	0.274	11.4	16.2
9	0.252	10.5	16.8
10	0.233	9.7	17.3
11	0.219	9.1	17.8
12	0.205	8.5	18.2
13	0.194	8.1	18.7
14	0.184	7.7	19.1
15	0.177	7.4	19.7
16	0.168	7.0	19.8
17	0.16	6.7	20.2
18	0.154	6.4	20.6
19	0.148	6.2	20.8
20	0.143	6.0	21.2
25	0.122	5.1	22.6
30	0.107	4.5	23.8

Table 1: Stoll and Chianta Data Points

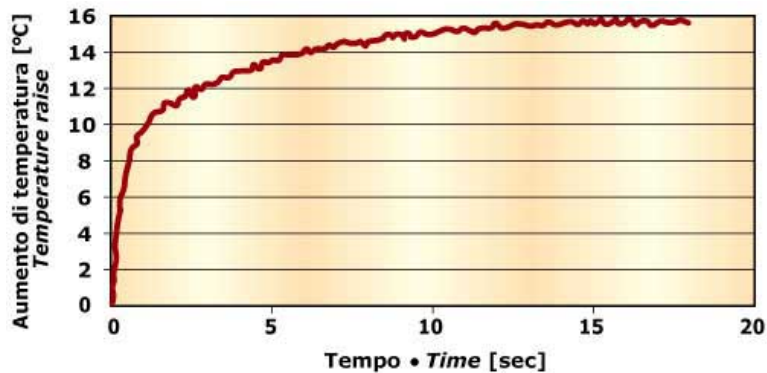


Figure 3: Stoll and Chianta Curve

These tests may also be conducted on a bench-top scale, using controlled sources of convective heat, radiant heat, or a combination of both. Once the level of heat energy from the source is known, fabric systems can be placed just in front of the sensor. Then, the amount by which the fabric prevents the heat energy from reaching the sensor is recorded, which is a measure of its thermal protective performance (Stoll and Chianta, 1969).

This protection factor may be expressed in kW/m² (cal/cm²), and the larger this number, the greater the protection factor of the fabric system. This allows different fabric systems to be rated in terms of their relative thermal protective performance.

In addition to testing fabrics on a bench-top scale, theory has been extended to the testing of garment systems on manikins such as the DuPont Thermo-Man® or our own “Bob” which are both instrumented with calorimeter sensors, linked to computer software for recording, organizing, and further analysis of the data.

Neither the Henrique Burn Integral nor the Stoll and Chianta method take into account the perspiration beneath a firefighter’s turnout gear.

2.1.4 Scald Burns

In the case of firefighters on duty, scald burns are generally second to third degree burns. Scald burns occur when external heat causes moisture inside a firefighter’s turnout suit to heat temperatures up to the point before water evaporates (Torvie, Hadjisophocieous, 1997). The resulting heated water burns the firefighter over a period of time which ends with the firefighter sustaining burns to their body.

This transport phenomenon is due to the water against the skin not allowing the body heat to evaporate. If the water against the skin is hotter than the temperature of the skin, then the heat cannot transfer away from the skin. With a barrier (aramid Nomex® material or cotton undergarment) blocking the evaporation of the water, the skin will not cool and in essence will burn. If hot air were just touching the skin and no water, then sweat will still be able to evaporate cooling the body (Cankar, 2002).

The most common areas to be burned on a firefighter are the hands, shoulders, biceps and knees. Within these four areas, the most likely to receive scald burns are the shoulders and biceps. The shoulders and biceps are common places for sweat to gather both because of human physiology and the turnout suits firefighters wear. Lawson observed that “sweat from the head and neck tends to collect in fabrics at a fire fighter’s shoulders” (1996). In addition, the SCBA (Self-Contained Breathing Apparatus) goes from the shoulders across the biceps. Because of this, perspiration tends to gather around the SCBA strap.

Moisture is usually present within a firefighter's turnout suit because he or she perspires from setting up equipment at the destination of the fire and from fighting the fire itself. From all these strenuous activities, the firefighters may be soaked with perspiration even before they start to fight the fire.

Firefighter protective clothing usually consist of two layers, an outer layer to prevent thermal injuries and an inner layer to reduce the passage of water (spray back from the hose). Lawson noted that the outer shell was created to resist "ignition upon being exposed to thermal radiation over very short periods of direct flame contact" (1996). The inner layer may also consist of an extra thermal barrier as well as a moisture barrier (Lawson, 1996). Because the moisture barrier prevents the passage of liquid or vapor, when a firefighter's suit is wet, it stays wet for the entirety of the firefighting session. Although the thermal barrier will slow the transfer of heat between the fire and the firefighter, prolonged exposure will still cause the turnout suit and the moisture within the suit to heat up (Lawson, 1996).

Furthermore, moisture in the cloth may vaporize upon heating and then recondense on the interior of the cloth. Studies performed by Prasad, Twilley and Lawson observed that the temperature of the fabric layers and total heat flux to the skin is significantly influenced by the amount of moisture and the distribution of moisture in the protective clothing (2002). This data clearly correlates with the information presented above by Lawson where thermal barriers and their impacts are analyzed.

2.2 Fire Protective Clothing

Fire protective clothing is produced in many forms; from children's sleepwear to fighter pilot's jumpsuits. These materials are sprayed with fire retardant or woven with fire retardant materials to reduce the chance of ignition on the clothing. Firefighters endure higher levels of heat and so more layers and specialized clothing have been developed.

The main protection a firefighter has from the intense heat and flame is his suit, or turnout. These specially made garments are tested under strict regulations to ensure they meet requirements set in NFPA 1971. A turnout is comprised of three layers, the top being the outer shell, followed by a moisture barrier and then the thermal liner on the inside. Although each turnout item adheres to standards there are many variations in materials used to make each layer. These variations allow fire fighters to choose the suit best for them and their situation, such as wild life fire or structural fires.

The clothing that was provided for this project was NOMEX® brand fiber, 99% Aramid and 1% Static Dissipative Fiber. This can be approximated as NOMEX® Material Aramid Type 430, for which the thermal properties are known to be as the density 1.38 kg/m³, the specific heat (25°C) 1213 J/(kg-K), and the thermal conductivity 0.12W/(m-K) (DeCristofano & Hoke, 1997).

To test these different fire protective materials, there can be large scale or small scale testing done. Large scale testing tests the system, which includes the entire turnout suit and possibly SCBA, headgear, and boots. Small scale testing tests a sample of material from the suit or just a piece of the system of a turnout suit.

2.3 Testing Methods for Fire Fighting Clothing

Currently, up-to-date and trustworthy test methods for firefighting clothing have been published by many different associations around the world. Some of the most known and used methods are those suggested by the NFPA code and ASTM. The main differences between these approaches focus mostly on the type of garment tested and the individual benchmarks on how to compare one sample to another (Hoschke, 2001). As a result none of these tests can be considered absolute.

To measure the temperature that reaches the skin, various acquisition devices can be used. The sensors provided for this project included copper slugs and glass-epoxy

composite sensors. Both devices have their strengths which will be discussed in the next section.

2.3.1 Thermal Sensors

All thermal sensors were run using LabView v7.0 that reported temperature readings in degrees Celsius. Copper slugs and glass-epoxy composite sensors were used throughout this project's testing.

2.3.1.1 Copper Slugs

The copper slugs provided were hand made in 2004 through a Masters Thesis at Worcester Polytechnic Institute. They were found to be the most inexpensive solution with the most positive attributes for predicting a second-degree burn. It should be noted that the temperature of skin rises more rapidly than the copper slugs can measure, therefore the calculated heat flux from these sensors does not perfectly represent the heat flux imposed upon the skin (Sipe, 2004).

The copper slugs were constructed out of Copper 110 alloy with a T-type thermocouple at the top. The thermocouple bead connects the bottom of the copper disk and the wire leads to the base of the copper slug. The copper disk thickness is reported to be accurate within 0.016 mm and the temperature is reported to be accurate within 3°C. (Sipe, 2004)

2.3.1.2 Epoxy-Glass Composite Sensors

The epoxy-glass composite sensors are composed of a 60/40 mixture by weight of alpha-cellulose-filled urea formaldehyde and silica. They are approximately 1.5 cm tall and 2.5 cm in diameter and are reported to have thermal properties similar to those of human skin. The measuring device inside the epoxy-glass composite sensors is a thermistor which works by measuring the change in resistance from the change in temperature.

The manufacturer specified a 3% tolerance on the device but through our research it was found that the epoxy-glass composite sensors, in fact, had a tolerance well beyond this. The average temperature discrepancy was found 0.1°C (Kimball, 1993). Dr Ned Keltner and Dr. Roger Parry are both scientists who have used these sensors in testing and have been involved with developing methods to calibrate them. From personal communication with them, they cited a large variation in accuracy and do not recommend using these without calibration first (Dr. Ned Keltner, personal communication, March 28, 2007) (Dr. Roger Parry, personal communication, February 7, 2007). Developing a calibration method for this project was out of scope and would be a lengthy process. Before testing was conducted for this project, it was not known that calibration would be necessary.

2.3.2 Possible Large Scale Tests

In real world situations, firefighters struggle not only with fire, but also with more determinant and “hard to reproduce” factors such as punctures, cuts or holes in the fire suits, lack of visibility while on duty which then hinders mobility...etc. This is one of the reasons why heat transfer through garment assemblies is one of the most significant properties (and easiest to test) when considering the effectiveness of fire fighting suits (Hoschke, 2001). Something to take in consideration is that the “protection rate” obtained in laboratory evaluations do not correspond to equivalent “protection rate” in field use (Hoschke, 2001). Consequently, it would be reasonable to consider this discrepancy when testing/comparing lab results.

2.3.2.1 Manikins

Manikin tests usually cost more than bench tests but yield better and more accurate results due to the control you have over the experiment. Some of the elements that increase the expenses in manikin tests are the manikin itself, the test room needed in order to perform this test, and the specialized equipment needed in order to operate the manikin.

2.3.2.1.1 Thermo-Man®

The Thermo-Man® is the most known manikin test method for fire tests. The DuPont THERMO-MAN® is an instrumented, six-foot, one-inch tall, high-temperature manikin system with 122 heat sensors specifically distributed along its body according to the isothermal body lines (E. I. du Pont de Nemours and Company). The THERMO-MAN® is dressed in complete turnout garments and engulfed in flames so that factors like garment construction, fabric weight, material type, style, fit and the impact of outerwear and undergarments can be taken into account.

This manikin is similar to a traversing manikin which has been provided for this project. However, there are only 44 sensors provided and not 122 sensors.

2.3.2.1.2 ASTM F1930: Standard Test Method for Evaluation of Flame Resistant Clothing for Protection against Flash Fire Stimulation Using an Instrumented Mannequin

This is a full-scale manikin test designed to test fabrics in completed garment form in a simulated flash fire. The manikin used is very similar to the Thermo-Man®, the only differences being that this one has less sensors and the shape of the garment used. Tests are usually conducted at a heat flux of 75.4 kW/m^2 ($1.8\text{-}2 \text{ cal/cm}^2\text{sec}$) and for durations of 2.5 to 5.0 seconds for single layer garments. Results are reported in percentage of body burn (ASTM, 2007).

For consistency in data and accuracy of comparison, the test method defines a standard garment size and configuration that must be used for each test. This is very important because manikin test results are heavily dependent on garment fit and design. The standard manikin test is not specifically designed to evaluate the protective performance of specific garment designs, although the test can also be used in this manner (ASTM, 2007).

The ASTM manikin test method was published very recently, and is just now being used by industry. Some of the manikin test data used in the industry today was generated in "non-standard" ways. Different organizations used varying test procedures

that affect results (for example, testing with and without underwear, different garment fits and styles). It is, therefore, very difficult to compare different manufacturers' manikin test data at this time.

2.3.2.1.3 Thermo-Leg®

The Thermo-Leg® test has the same functionality that the Thermo-Man® test except for one feature; it was designed to illustrate and mimic the movement of a firefighter wearing his/her garment under real fire conditions (Behnke et al., 1992).

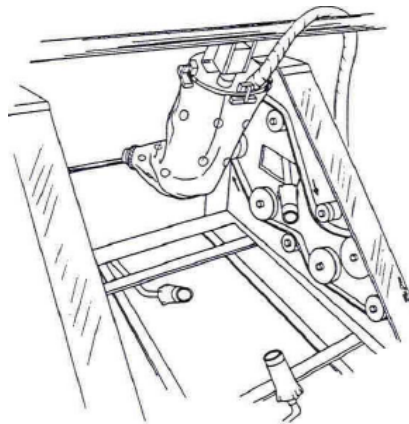


Figure 4: Illustration of Thermo-Leg (R) Test

The Thermo-Leg® test is set up by swinging the leg on a controlled pendulum while four propane burners heat the area. The leg has the same allocation of sensors as the Thermo-Man® test and also the same material composition. A diagram of the Thermo-Leg® test can be seen in Figure 4.

2.3.3 Possible Small Scale Tests

Different test methods have been developed to test and stress the value of a garment. Some of the most common ones are the Vertical Flammability Test (ASTM D-6413), The Thermal Stability Test, and The Thermal Shrinkage Test. Even though these tests indicate what kind of conditions a garment can withstand while in field, they do not offer any real significance to the purpose of our research, therefore, they will not be taken

into account. Instead, small scale tests, also known as bench-scale tests, which measure the properties of the materials, are discussed.

2.3.3.1 Test for Thermal Protection Performance (TPP)/ ASTM D4108-87

The Thermal Protection Performance Test (TPP) predicts the amount of thermal protection a fire resistant (FR) fabric would provide if exposed to a flash fire (E. I. du Pont de Nemours and Company, 2006). The TPP value is defined when the exposed energy on the outside of the fabric has enough energy to pass through the fabric and cause the onset of a second-degree burn if a person was wearing the fabric (E. I. du Pont de Nemours and Company, 2006). Second-degree burns are used in this examination as test-benchmarks because they are easy to identify due to the visible effect of blistering in the skin (E. I. du Pont de Nemours and Company, 2006).

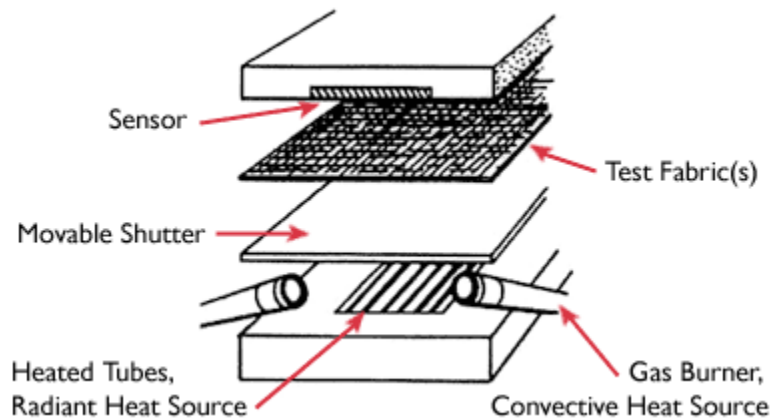


Figure 5: Layers of Thermal Barriers

The way this test reflects how protective a fabric is, is by assigning a rating number to each of the tested samples. Therefore, the higher the TPP value, the more protective the fabric is. Currently, there are two ways to test a fabric for TPP. One is called the “spaced TPP” and the other one is called “contact TPP”. In spaced TPP, fabrics are tested with a space gap (1/4”) between the test samples and the heat sensor to measure the fabrics' ability to provide a barrier between the heat source and the skin. For the

contact TPP test, fabrics are tested in contact with the heat sensor to measure the fabrics' ability to provide thermal insulation (E. I. du Pont de Nemours and Company, 2006).

2.3.3.2 Test for Radiant Protective Performance (RPP)/ ASTM F1939-99A

The RPP test is in essence exactly the same as the TPP test, with the only difference that the heat source in a RPP test is 100% radiant heat. The definition for the RPP test is “the amount of a radiant heat energy required to cause a second degree burn when a person is wearing the tested fabric” (E. I. du Pont de Nemours and Company, 2006). As with the TPP test, the higher the RPP test, the more protective the fabric is.

2.3.3.3 Cone Calorimeter Testing

To simulate properties that are identified in large scale tests in a heated environment, the cone calorimeter is often used. The cone calorimeter has a heating device that directs the heat to a 0.11 m by 0.11 m area located below it. This apparatus can measure the heat flux, the total heat released, the effective heat of combustion, the time to ignition, smoke obscuration, mass loss rate, and the total mass loss (WPI, 2006).

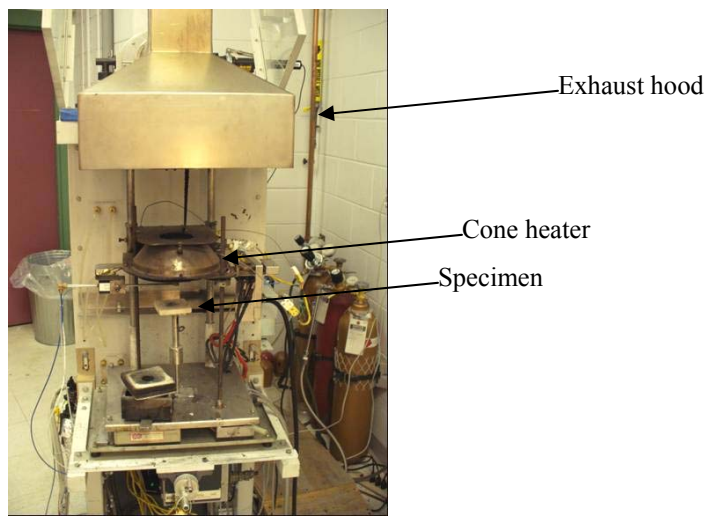


Figure 6: Cone Calorimeter

The data collected from the cone calorimeter is done by a computer running a LabView program.

2.4 Past Moisture Study

There are a few studies to date that have looked into the effect of moisture from perspiration on the thermal capabilities of turnout gear. One such study was done by The Center for Research on Textile Protection and Comfort (T-PACC) at North Carolina State University. The study looked into the TPP test results of firefighter protective clothing pretreated with moisture in a low level heat exposure (T-PACC, 2001).

2.4.1 Moisture Absorption in Turnout Garments

Before the TPP test was conducted, research was done on the location and amount of moisture produced from perspiration. Physiological studies showed that a majority of moisture absorption happened in the undergarments worn beneath the turnout garments. The breakdown came out to excess of 90% saturation in undergarments as compared to 1.5%-15% in turnout gear (T-PACC, 2001).

The amount of moisture absorbed into the turnout garment depends on the fabrics used. Some thermal liners wick moisture away from the body better than others. Another factor is the breathe ability of the moisture barrier. Breathable moisture barriers prevent moisture build up in the thermal liner by allowing evaporation to occur (T-PACC, 2001). Figure 7 shows the results of different configurations of thermal liners and moisture barriers as compared to moisture build up in different items worn during fire fighting.

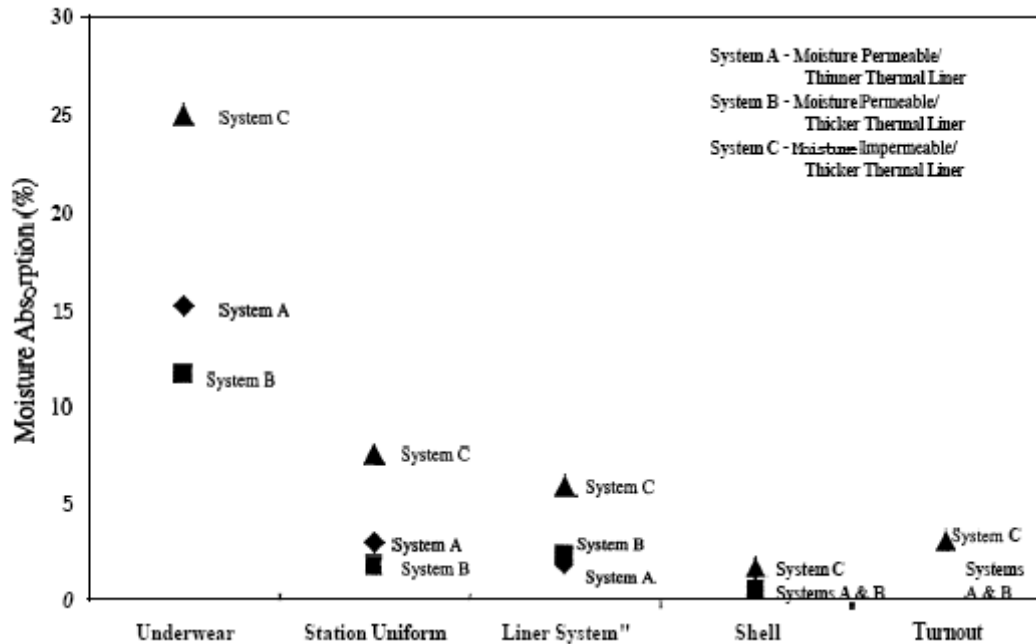


Figure 7: Effect of Moisture Barrier Permeability and Thermal Liner and Sweat Accumulation in Firefighter Clothing in Wear

The results of this test showed that impermeable moisture barriers in general allow more moisture to build up in undergarments because it prevents the transport of moisture through evaporation (T-PACC, 2001).

2.4.2 Moisture Transport in Turnouts

As stated above, evaporation is one method by which moisture is picked up in turnout gear; the other is through direct contact with wet skin. T-PACC conducted two experiments to understand which method best portrays the moisture transport system in actual fire fighter gear. The results showed that evaporation more closely produced saturation levels similar to those found in wear. Wicking of moisture through direct contact can only be applied in situations where the thermal liner is in direct contact with the skin. It is important to understand how much moisture is absorbed by turnout garments in order to accurately develop a system to precondition tested gear (T-PACC, 2001).

2.4.3 Developed Preconditioning Protocol

T-PACC developed a system to precondition test specimens in order to accurately simulate a moisture laden turnout. The protocol involves precisely weighing the specimen, then spraying the facecloth side of the thermal liner with water until the specimen's weight has increased by approximately 15%. As recalled from above, 15% is the high end of the range of percent absorbed in turnout gear as found in wear trials. The specimen is then sealed in a plastic bag and left to condition for at least 12 hours. After that period, specimens are taken out of the bag and weighed again. T-PACC ran many trials of this protocol and found it to be consistent with the amount of moisture found in each specimen. Also, moisture gradients in each layer of the turnout specimens were consistent with wear trial gradients (T-PACC, 2001).

2.4.4 T-PACC Testing

T-PACC ran tests on a turnouts consisting of a 254 g/m² Kevlar®/PBI outer shell, Crosstech® on Nomex® pajama check moisture barrier, and Aralite® thermal liner. The preconditioning protocol described above was followed with the exception that the specimen was sprayed to a 100% increase in weight. Figure 8 shows the setup for their testing. The specimen was exposed to heat ranging from 6.3 to 21 kW/m² (T-PACC, 2001).

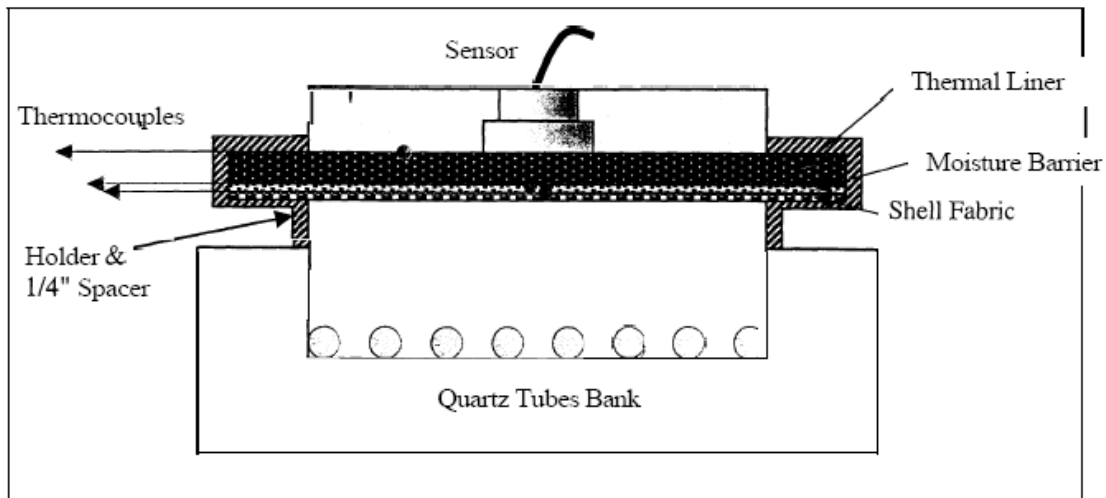


Figure 8: Setup for T-PACC Testing

The tests run by T-PACC showed that the thermal protective performance of the permeable test specimen increased when wet. The test indicates that moisture has the effect of reducing transmitted heat energy. Figure 9 shows a comparison of wet and dry test specimens at different heat exposures (T-PACC, 2001).

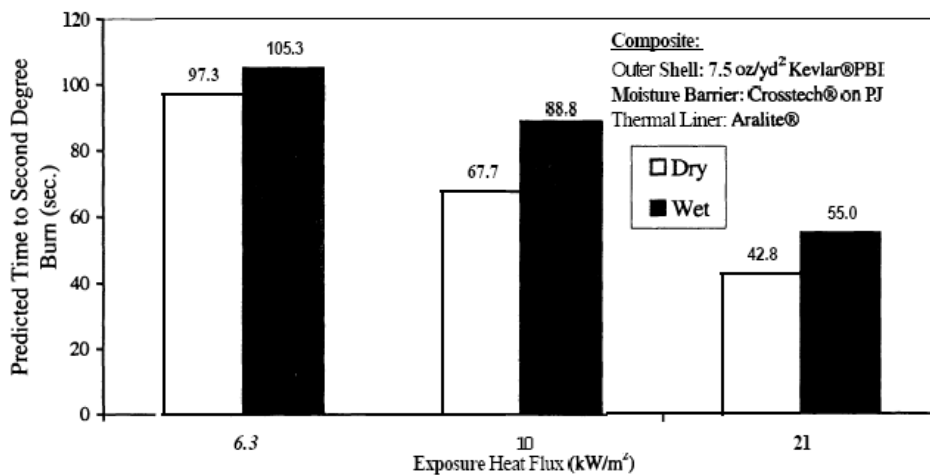


Figure 9: Comparison of Wet and Dry Specimen using T-PACC

Information regarding scald burns, testing methods, and previous research was discussed in this chapter. The following sections were based on this research and may refer back to this chapter.

3 Methodology

The goal of this project was to *determine if scald burns could be tested in a lab setting to further facilitate future research with functional guidelines*. In attempt to accomplish this goal, four objectives were devised and executed. In this chapter, the methods that were used in attempt to fulfill our goal are discussed.

The first objective was to set up a list of *possible* testing methods that could yield valuable information regarding scald burns. The second objective was to create a lab procedure for both test methods that will mimic a wet undergarment on a firefighter. A detailed lab procedure may greatly increase the accuracy within our own experiments as well as that of future research. Also, with a detailed procedure it may be easier to identify the dependent and independent variables of the given test. The third objective involved comparing both wet and dry test results to theoretical equations in order to examine the physical process of the test and the extent of the burns. Lastly, the different types of thermal sensors used in the project were compared to determine if the model derived by M.S Joel Sipe that does not account for the moisture barrier could be used in an environment with a moisture barrier.

3.1 Possible Test Methods

To find the appropriate test method for the large- and small-scale testing, the test methods were researched and then compared with a “Positives” and “Negatives” list. Possible test methods for the large-scale testing can be seen in Table 2.

Large-Scale Test Method	Positives	Negatives
Thermo-Man®	<ul style="list-style-type: none"> • 122 sensors located on isothermal body lines • Made to withstand high temperatures • Can be tested in complete turnout gear 	
ASTM F1930	<ul style="list-style-type: none"> • Typical heat flux set to 75.4 kW/m² 	<ul style="list-style-type: none"> • Results reported in amount of body burned • Standard size of garment must be used • Fewer than 122 sensors
Thermo-Leg®	<ul style="list-style-type: none"> • Sensors located along isothermal body lines (same amount as Thermo-Man® has in one leg) • Made of material to withstand high temperatures 	<ul style="list-style-type: none"> • Swings in and out of flame to mimic a firefighter's movements

Table 2: Comparison of Different Large-Scale Test Methods

It was found that the use of a fully dressed Thermo-Man® manikin, or alike, equipped with sensors, should be used for this procedure. Since the goal of the project was to determine whether scald burns could be tested in a laboratory setting; using tests like the thermo-leg which comprise only a specific section of the body would yield on results which are insufficient to achieve our goal. That is the main reason why a full manikin was needed to perform the full scale test.

For the project a different procedure than the one established by DuPont's Thermo-man was used. There are two main reasons for this decision. The first one is that we wanted to expose the fabrics over the manikin to a more realistic environment where flames would come from the floor and not as turrets from all the directing. The intention of the project was not to test wildfire clothing in flashover-like conditions.

The second reason was more of a giveaway; the lab at Holden, Massachusetts already had a traversing manikin installed and ready to be used. For the best interest of the project this saved money, resources and time.

Small-Scale Test Method	Positives	Negatives
TPP (ASTM D4108-87)	<ul style="list-style-type: none"> • Predicts amount of thermal protection a fire resistant fabric would provide if exposed to a flash fire 	<ul style="list-style-type: none"> • Second degree burn is the test benchmark (ie. Does not test for first degree burns) • Outputs a “TPP value” which is a rating
RPP (ASTM F1939-99A)	<ul style="list-style-type: none"> • Predicts amount of radiation protection a fire resistant fabric would provide if exposed to a flash fire 	<ul style="list-style-type: none"> • Only radiant heating • Second degree burn is the test benchmark (ie. Does not test for first degree burns) • Outputs a “RPP value” which is a rating
Cone Calorimeter	<ul style="list-style-type: none"> • Can measure: <ul style="list-style-type: none"> ○ Heat flux ○ Total heat released ○ Effective heat of combustion ○ Time to ignition ○ Smoke obscuration ○ Mass loss rate ○ Total mass loss • Can reach up to 13.1 MJ/kg of oxygen consumed 	<ul style="list-style-type: none"> • Need a method to analyze outputted data

Table 3: Comparison of Different Small-Scale Test Methods

It was found that the use of the Cone Calorimeter, should be used for the small scale testing. Other tests such as the TPP or the RPP predict specific properties of the fire fighter clothing when exposed to heat fluxes. These tests don’t provide any information regarding the skins reaction to heat fluxes or whether it will receive a second degree scald burn; that’s why they can’t be used. The cone calorimeter is the only small scale test that could be adapted to the needs of the project.

3.2 Laboratory Testing Procedures of Manikin

Testing was conducted in Alden Laboratories at 85 Shrewsbury Street in Holden, Massachusetts. To test in this laboratory, the procedure provided by the report entitled Thermal Manikin Testing of Fire Fighter Ensembles, as outlined in Appendix B, was used; this includes safety checks, proper use of equipment, and shut down operations.

3.3 Materials Testing Procedure

Similar procedures were used for testing the dry and wet undergarments. The method for testing dry materials is outlined first and then the testing for wet materials can be inserted between steps 6 and 7.

3.3.1 Dry Materials

To prepare the manikin for testing dry undergarments, the following procedure was implemented:

1. While manikin is hanging on guide track, clothe manikin in a pair of men's briefs underwear and pull fire resistant pants onto legs.
2. Slice back of pants near belt loop approximately 3 inches down. This is to allow the bundle of thermocouple cords to run down the back of the manikin.
3. Secure the bundle of thermocouple cords in place by running a single thermocouple cord through the belt loops and around the bundle and twisting the two ends together in the front until the bundle and pants are snug in place.



Figure 10: Thermocouple belt around the waist of manikin

4. Pull boots onto manikin's feet and tie shoelaces.
5. Remove manikin from guide track
6. Unhinge arms from sockets.
7. Clothe manikin in a men's large white undershirt (as seen in Figure 11) and carefully pull on fire resistant jersey.



Figure 11: Dressing manikin in large white cotton undershirt

8. Tuck shirt into pants, underneath thermocouple belt so ends of jersey is sealed in pants and no undershirt is visible.
9. Replace arms and tighten.
10. Hang manikin in place on guide track and tighten bolts.

3.3.2 Wet Materials

To test wet undergarments the following supplemental procedure may be inserted between step 6 and step 7.

1. Fill a container with 248 mL.
2. Pour the bottle into a mop bucket attempting to evenly distribute water amongst the basin.



Figure 12: Pour water into bucket

3. Lay the undershirt into the bucket so that it is half-immersed.



Figure 13: Half-immersed undershirt in water

4. Wait for the water to be absorbed into the cloth, and then immerse the other half of the undershirt.
5. Identify areas that are dry and wet those areas with water remaining in bucket.
6. Once undershirt is completely wet, ring the undershirt until there are no drips.



Figure 14: Ring wet undershirt until there are no drips

3.4 Cone Calorimeter Testing Procedure

To help complete our fourth objective of comparing the temperatures of the sensors when using wet and dry undergarments, cone calorimeter testing was conducted. Four sets of testing were conducted, each with a specific goal. The first set of tests was conducted to mimic the full scale tests; using a high heat flux for a short period of time. These first tests were conducted with both the epoxy-glass composite sensors and the copper slugs. The second set of tests was conducted to identify the curve that the epoxy-glass composite sensors produce at a low heat flux over a long period of time. This testing was only done with the glass-epoxy composite sensors. The third set of tests used both the epoxy-glass composite sensors and the copper slugs. They were conducted with cloth samples, wet and dry, with low heat flux over long period of time. The fourth set of

tests was similar to the third tests except they used only copper slugs. From our research, it was found that most scald burns occur at low temperatures over an extended period.

3.4.1 First Tests: Glass-Epoxy Composite Sensors and Copper Slugs

The sensors used in the full scale testing were epoxy-glass composite with little known information about their readings. To help relate the epoxy-glass sensors to information that was known, they were tested with the copper slugs at various high heat fluxes. All of the epoxy-glass composite sensors and all of the copper slugs were tested with the following procedure.

1. Set cone calorimeter to read 293°C. This is approximately 5 kW/m².
2. Once cone calorimeter reads this temperature and stays steady for approximately five minutes, then testing is ready to begin.
3. Insert sensor into fiberboard substrate, place sample on top of this (see Figure 15), and connect sensor to thermocouple clip.

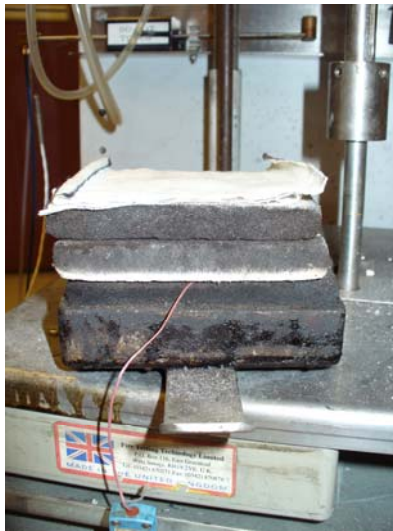


**Figure 15: Sensor inside fiberboard substrate with sample on top.
(Notice the thermocouple clip hanging outside of the assembly.)**

4. Place metal encasing onto sensor assembly (see Figure 16) and place this onto the stand under the cone heater. Make sure that top of assembly is 2.54 cm away from the bottom of the cone heater.



Figure 16: Assembly ready to be placed on stand

5. All at the same time, begin stopwatch, open damper, and run the LabView program.
6. After 390 seconds, all at the same time, stop stopwatch, close damper, and stop the LabView program.
7. Change the sensor and repeat testing for all sensors until all have been tested at the following heat fluxes, 5 kW/m²(293°C), 10 kW/m²(390°C), 15 kW/m²(462°C), 20 kW/m²(529°C), and 25 kW/m²(580°C).

3.4.2 Second Tests: Glass-Epoxy Composite Sensors at Low Heat Fluxes

With scald research indicating that most burns occur at low heat fluxes over long periods of time, the epoxy-glass composite sensors were tested in the cone calorimeter as such. The procedure for the first test was also used in this testing except for the following values for 390 seconds.

Heat Flux	Temperature Reading on Cone Calorimeter
1 kW/m ²	175°C
3 kW/m ²	218°C
5 kW/m ²	293°C

Table 4: Heat Fluxes Used in Second Tests

3.4.3 Third Tests: Wet and Dry Cloth Samples for 390 Seconds

Cloth samples consist of aramid Nomex® material on the outer surface and a 100% cotton undershirt. The wet samples increased in weight by 29.4 mg because of the water added to the undershirt. This amount of water saturated the shirt, making it completely soaked without allowing water to drip off the shirt. Dry samples were at ambient temperature and did not undergo any conditioning.

The samples were contained in a metal casing on top of the sensors. The epoxy-glass composite sensors and the copper slugs were surrounded by a fiberboard substrate. An example of a sensor in the complete set up can be seen in Figure 15.

Both types of samples were tested using the same procedure in the first tests at 5 kW/m² for 390 seconds. After those tests concluded, the heat flux was raised to 10 kW/m² and the procedure was repeated for 390 seconds.

3.4.4 Fourth Tests: Wet and Dry Cloth Samples for 600/900 Seconds

Cloth samples consist of aramid Nomex® material on the outer surface and a 100% cotton undershirt. The wet samples consisted of the undershirt being soaked in 29.6 mL of water. This amount of water saturated the shirt, making it completely soaked without allowing water to drip off the shirt. Dry samples were at ambient temperature and did not undergo any conditioning.

The samples were contained in a metal casing on top of the sensors. The copper slugs were surrounded by a fiberboard substrate. An example of a sensor in the complete set up can be seen in Figure 15.

Both types of samples were tested using the same procedure in the first tests at 10 kW/m² for 600 and 900 seconds.

3.5 Developing Governing Equations

The third objective was to create a compare the wet and dry tests to determine if a burn occurred. In order to do this, theoretical governing equations were developed to understand what is occurring below the moisture barrier. This section develops these equations as well as illustrates the heat fluxes through the barrier.

3.5.1 Heat transfer through moistened clothing

The following equations demonstrate the theoretical process undergoing inside the moisture barrier of Figure 17.

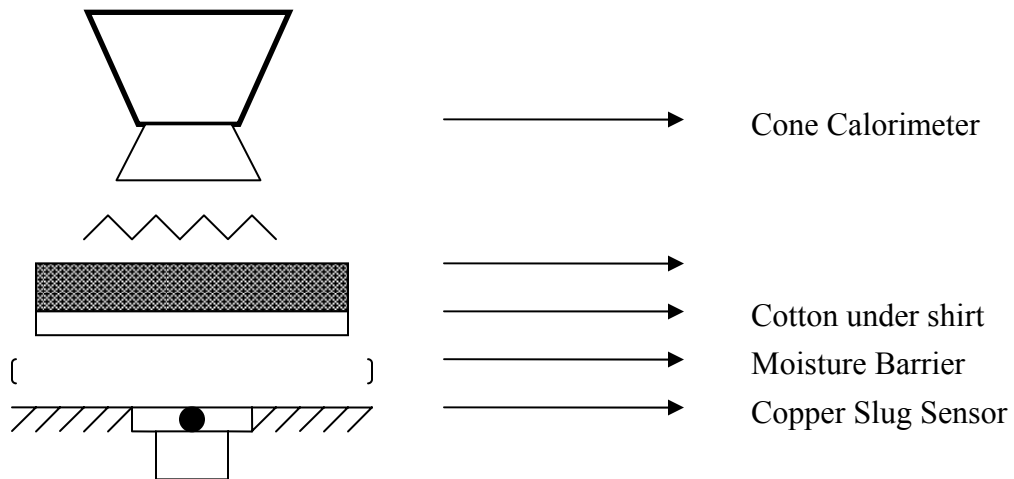


Figure 17: Illustration of Cone Calorimeter with Sample

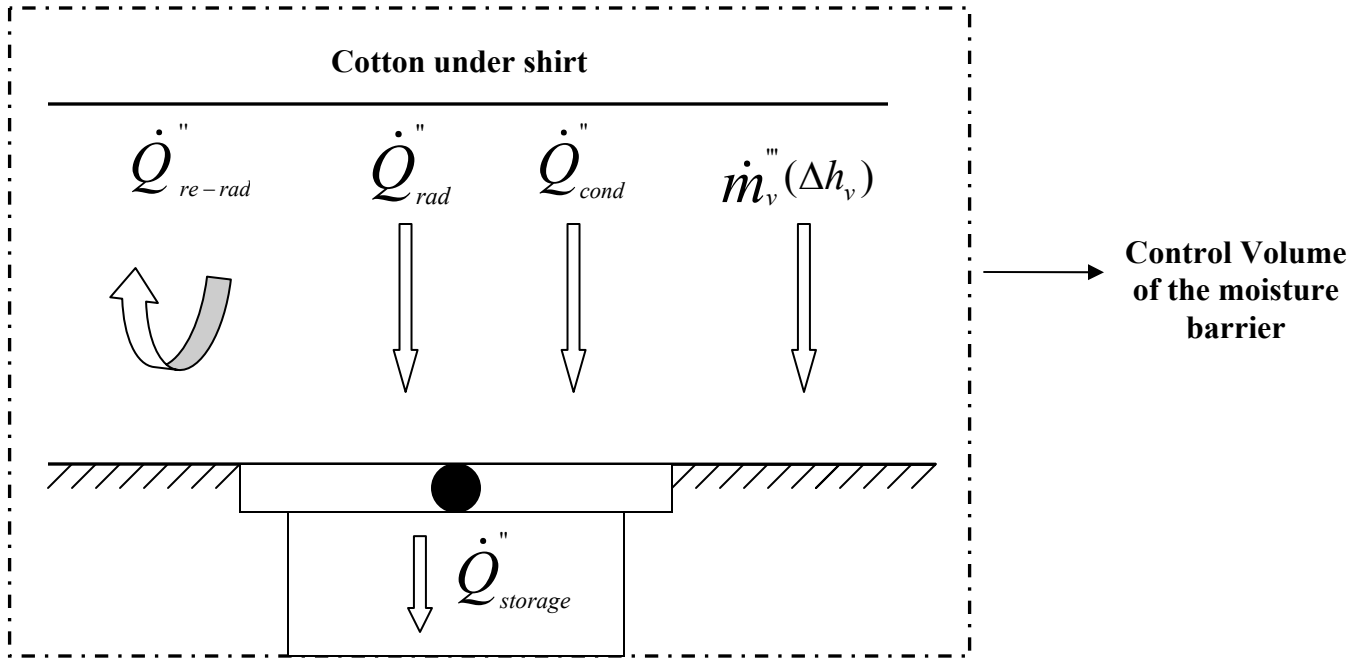


Figure 18: Control Volume of the Moisture Barrier

Assumptions:

- Transient conduction through fabric and moisture layer
- 1-D conduction (only in the z-axis)
- \dot{Q}''_{re-rad} term can be neglected due to the relative low temperatures at which the skin is.
- Fabric is uniformly moistened; therefore, we have a uniform \dot{Q}''_{cond} over the entire CV and a uniform thermal conductivity term over the control volume.

To begin the analysis, a control volume was drawn around the moisture barrier; this includes the lower portion of the cotton layer as the upper boundary and the sensor surrounded by insulated board as the lower boundary. The main purpose of drawing a control volume is to encompass all the necessary terms that act upon the physical process of a scald burn within a restricted limit.

Equation (1) depicts the energy balance performed over the control volume of the moisture barrier.

$$\dot{Q}_{rad}'' + \dot{Q}_{cond}'' = \dot{Q}_{re-rad}'' + \dot{Q}_{storage}'' + \dot{m}_v'''(\Delta h_v) \quad (1)$$

Once the heat flux transmitted from the cone calorimeter to the fabrics reaches the moisture barrier, three different modes to convey heat can be observed. The first is a conductive heat flux, the second is a radiative heat flux, and the third is transmission due to the condensation process or phase change that water undergoes in the moisture layer.

The former conductive heat flux, radiative heat flux and heat transmission due to condensation will turn into one main term once it reaches the sensor. It will turn into the storage heat flux.

Realizing that the radiative heat flux and the conductive heat flux can both be grouped into one term as shown in Equation (2), Equation (3) can be developed.

$$\dot{Q}_{incident}'' = \dot{Q}_{rad}'' + \dot{Q}_{cond}'' \quad (2)$$

$$\dot{Q}_{incident}'' = \dot{Q}_{re-rad}'' + \dot{Q}_{storage}'' + \dot{m}_v'''(\Delta h_v) \quad (3)$$

Each of the terms present in Equations (2) and (3) has their respective expression associated with them. This following section is devoted to understanding what each of these terms represent in each of the expressions. By better understand the general effect of moisture within fibers in presence of a fire, enhanced theoretical conclusions can be formed later from the gathered results.

The incident conductive heat flux is equal to the thermal conductivity of the wet fabric (k) multiplied by the change in temperature over the change in distance as shown in Equation (4).

$$\dot{Q}_{cond}'' = k \frac{\partial T}{\partial x} \quad (4)$$

Equation (5), the incident radiative heat flux is equal to the emissivity term of the cotton undershirt multiplied by the Stephan-Boltzmann Constant and the temperature

difference between the fabric's temperature and the skin's temperature. Both temperatures are elevated to the fourth power due to the intrinsic physics of radiation.

If the cotton undershirt was a perfectly emissive body then ε would be 1 but since it is not, the effects of heat over the cotton undershirt will have a dramatic impact on this term.

$$\dot{Q}_{rad}'' = \varepsilon\sigma(T_f^4 - T_s^4) \quad (5)$$

Equation (6), the storage heat rate is composed of the mass of skin in the control volume, times the specific heat of skin, times the time derivative of the skins temperature with respect to time.

$$\dot{Q}_{storage}'' = mc_p \frac{\partial T_s}{\partial t} \quad (6)$$

By realizing that density (ρ) is equal to mass (m) over volume (ℓ^3) and by replacing this into Equation (6), a storage heat flux can be developed. This is Equation (8).

$$\dot{Q}_{storage}'' = \ell\rho c_p \frac{\partial T_s}{\partial t} \quad (7)$$

Even though Equation (7) is quite simple and straight forward, it has the most significance to the project since all the skin burns due to water condensation will be reflected on its magnitude.

Equation (7) is equal to the length of the skin layer to be analyzed in order to perceive a 2nd degree burn multiplied by the density of the skin, the specific heat of skin, and the time derivative of the change in temperature difference.

A further theoretical derivation can be done once it is recognized that the density, the specific heat, and that thermal conductivity of the moisture barrier are actually dependant on the time and the temperature of the layer. As a result, they can be pulled

into their respective integrals and form Equation (8) which is the conjectural governing equation for one-dimensional heat transfer over a medium.

$$\rho c_p \frac{\partial T}{\partial t} = \frac{\partial}{\partial x} \left(k \frac{\partial T}{\partial x} \right) \quad (8)$$

The rate of condensation term plays an important role in determining a scald burn on the skin because it is the only term that takes into account the real effects of the moisture barrier. Equation (9), the rate of condensation, is equal to the volumetric flow rate of vaporization multiplied by the change in the latent heat of vaporization. The units of the rate of condensation are (W/m³) which means that it has units of power per volume.

$$\text{rate of condensation} = \dot{m}_v''' (\Delta h_v) \quad (9)$$

The methodologies discussed in this chapter were performed and the data was collected. With these equations, the results can be analyzed in the following section. It is important to note that

4 Results

4.1 Creating a curve to analyze the new sensors

In previous years, the Fire Lab in Holden, Massachusetts has used copper slug thermal sensors that can be analyzed with the Stoll and Chianta curve to determine if a second degree skin burn occurs. It was hoped that the same curve could be used to analyze data gathered using the epoxy-glass composite sensors which were provided by the Navy Textile and Research Center. Unfortunately, this was not the case. Figure 19 shows the time-temperature curve from one of the full-scale tests run at Fire Lab. The two sensors were located in the right and left collarbone areas on the manikin and the thermocouple was located in between them.

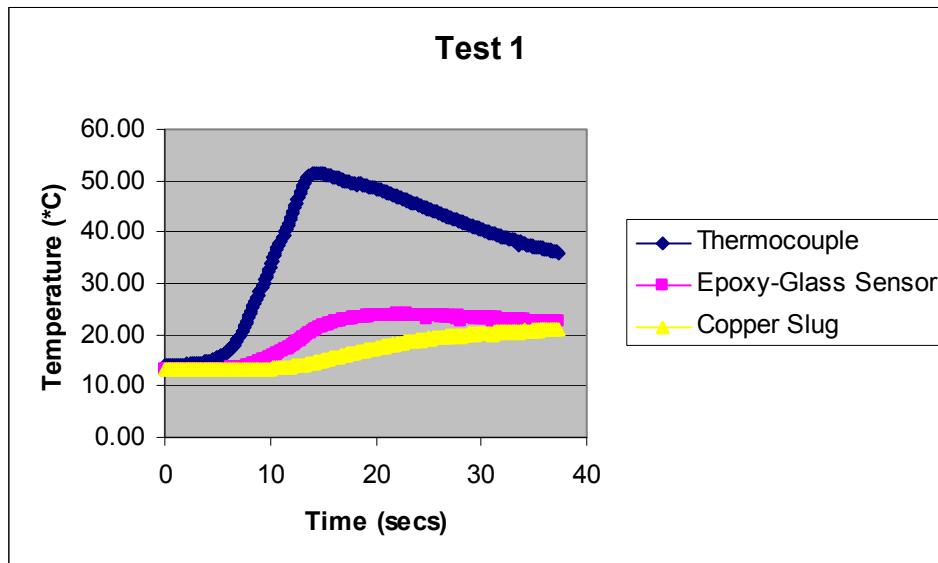


Figure 19: Sensor Comparison Full Scale Test

The epoxy-glass composite sensor has a time-temperature curve much different than the old sensor. Although the sensors reached the same overall temperature, burns occur from a rapid change in temperature. The Stoll and Chianta curve is based on change in temperature over time from the point when the sensor was first exposed to the heat insult. For Figure 19, that would be around 12-14 seconds, or the time it took the manikin to reach the door of the room from its starting point. The epoxy-glass composite

sensor records an instantaneous rise in temperature while the copper slug has a delayed, more gradual rise. As the curve was calibrated for copper slug sensors, it may falsely recognize more burns with the epoxy-glass composite sensors.

To reaffirm this, tests were conducted in the cone calorimeter in the lab at WPI. This way a constant heat flux could be applied to the different sensors and an accurate depiction of the difference in the sensors could be seen. The tests were conducted at 5, 10, 15, 20 and 25 kW/m² heat fluxes. The results were graphed with the Stoll and Chianta curve and it was found that there was a significant difference. The epoxy-glass composite sensors routinely showed a time-temperature curve that followed an exponential trend while the copper slug sensors rose linearly. Figure 20 through Figure 24 show the results from these tests.

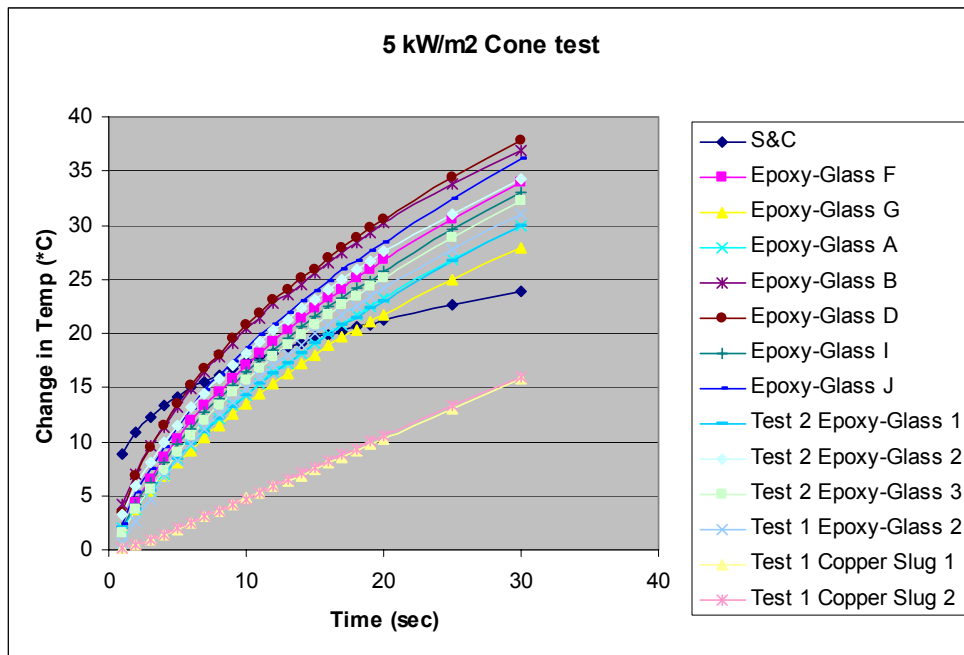


Figure 20: Cone Test Results (5 kW/m²)

In Figure 18 the data from the copper slugs do not intersect with the Stoll and Chianta curve. Since this curve was designed for these sensors, a curve for the epoxy-glass sensors needed to be developed with the same space relation to the sensor as the Stoll curve is to the copper slugs.

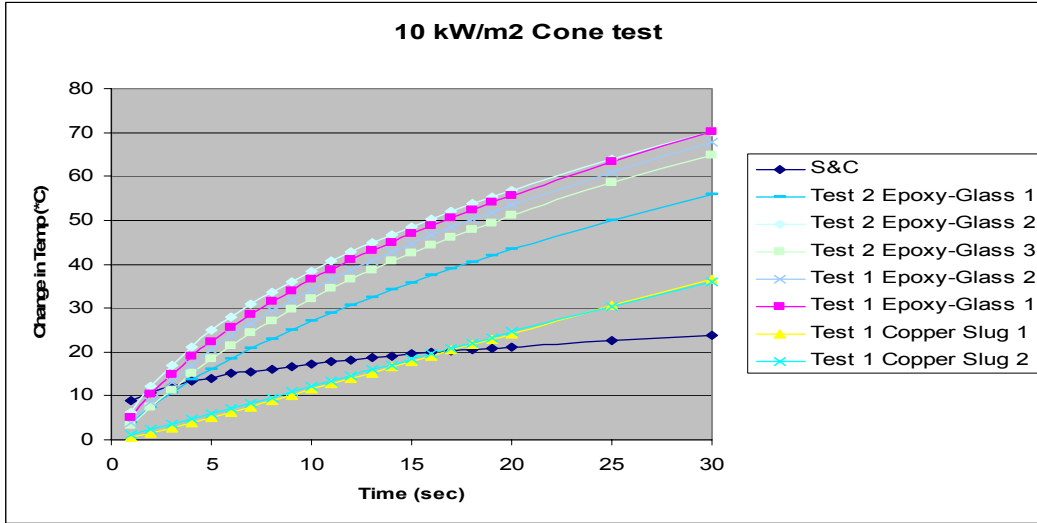


Figure 21: Cone Test Results (10kW/m²)

As the heat flux is increased the change in temperature versus time increases and soon the data intersects with the Stoll and Chianta curve. For a 10 kW/m² heat flux, the time to a burn is roughly 17 seconds. For the epoxy-glass analysis curve, described later, the Stoll and Chianta curve was translated so as to intersect the epoxy-glass data at 17 seconds.

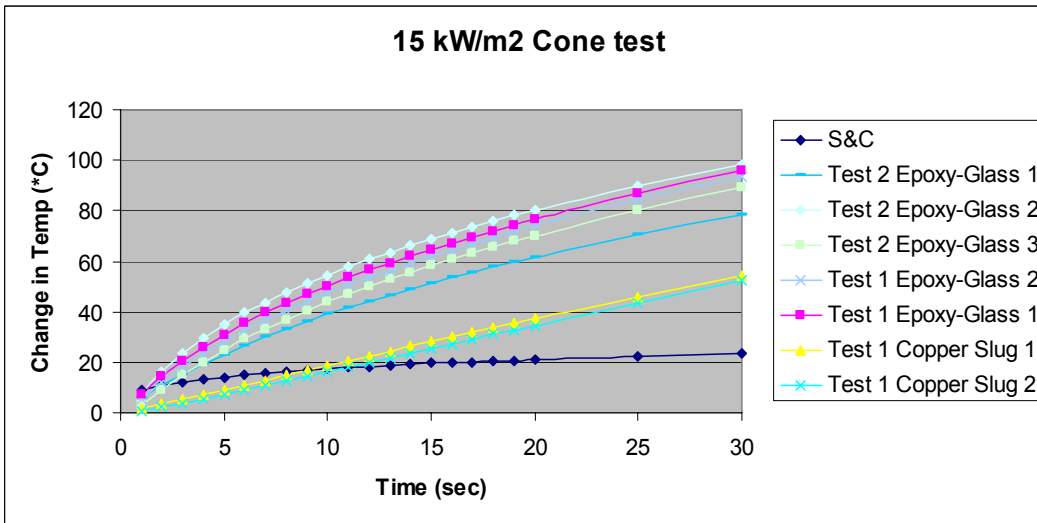


Figure 22: Cone Test Results (15 kW/m²)

As with the previous figure, figure 20 shows that a burn will occur at approximately 10 seconds at a 15 kW/m² heat flux. The epoxy-glass sensors rise in temperature so quickly that a burn is recorded instantaneously. Again for the new curve, as will be described latter, it was developed so as to intersect at this data at 10 seconds.

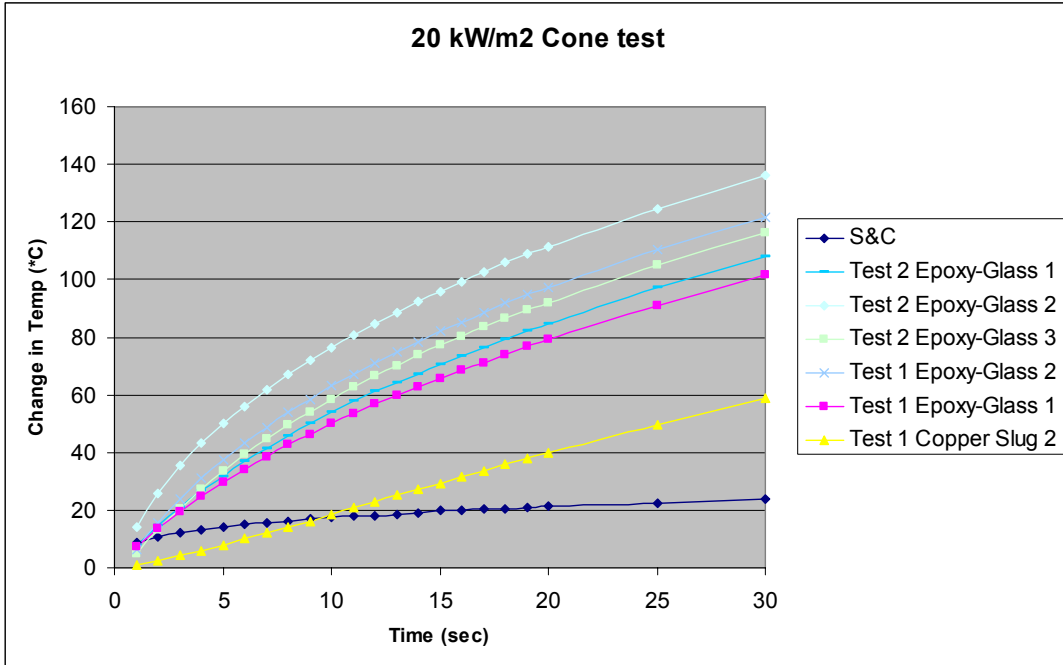


Figure 23: Cone Test Results (20 kW/m²)

The last three heat fluxes tested, showed that the substantial change in temperature with the epoxy-glass sensors when analyzed against the Stoll and Chianta curve produce an immediate burn. The copper slug data, on the other hand, demonstrates the more realistic analysis or a burn at 10 seconds (20 kW/m²) and 7 seconds (25 kW/m²).

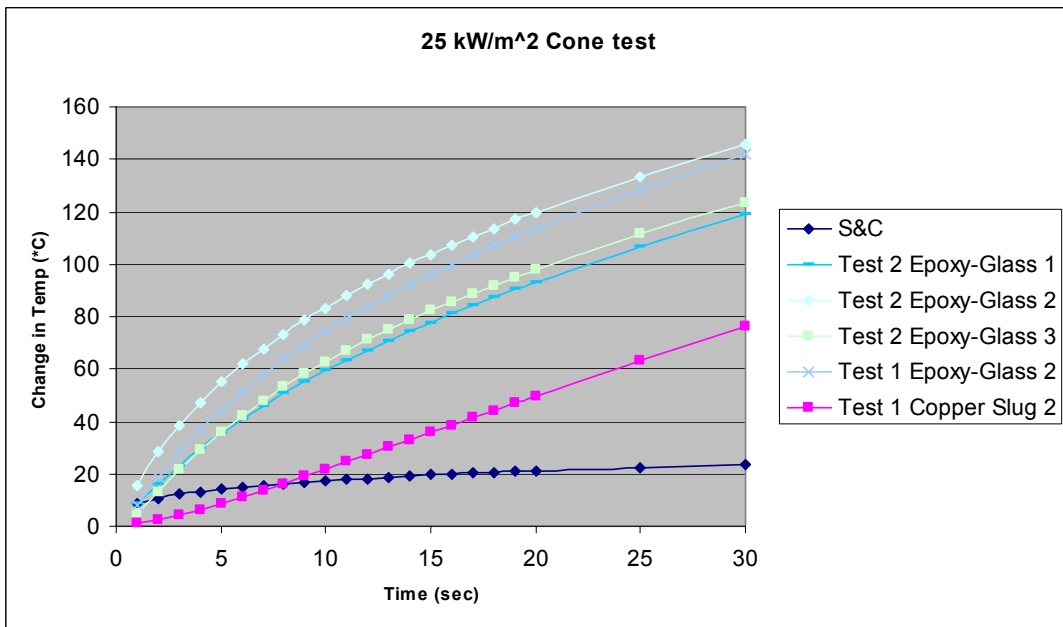


Figure 24: Cone Test Results (25 kW/m²)

After conducting these tests, it was determined that a way to analyze burns with the epoxy-glass composite sensors was needed to accurately analyze the full-scale test data. From the cone tests, a curve similar to the Stoll and Chianta curve was derived. The process to derive the new curve, involved averaging all of the epoxy-glass composite sensor temperature change versus time data for each heat flux. Next, the linear regression of the average was determined for each heat flux. Finally, the new curve was calculated by taking the difference between the Stoll and Chianta curve points and the average of the points from the copper slug sensor data, and adding it to the linear regression line points. This ensured that the new curve mimicked the interaction between the Stoll and Chianta curve and the copper slug data. The data from the epoxy-glass composite sensors would cross the new curve at the same time as the copper slugs do with the Stoll and Chianta curve for a given heat flux. Figure 25 demonstrates the process:

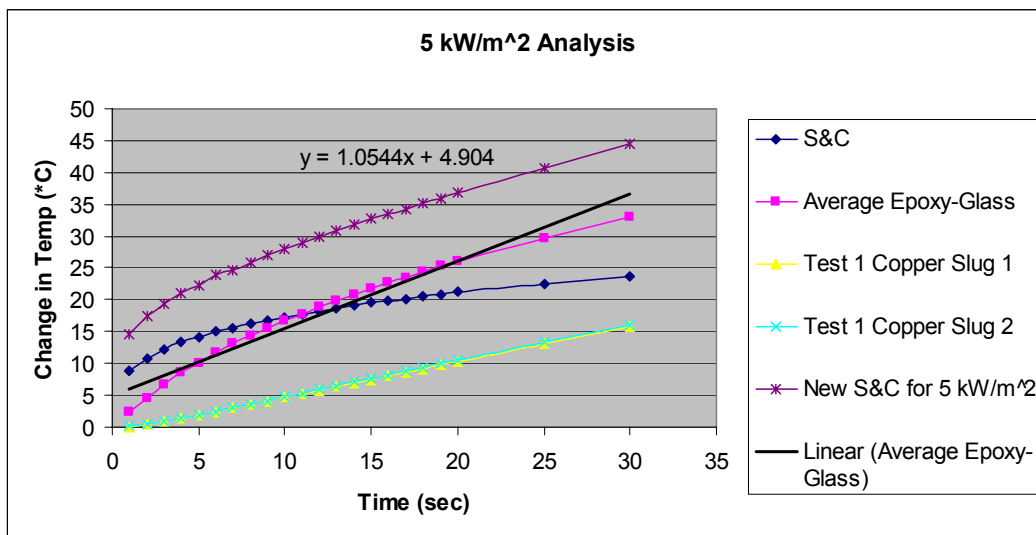


Figure 25: New Curve Derivation Process

This process was followed for all the heat fluxes previously mentioned (5, 10, 15, 20, 25 kW/m²). The points from the new curve derived at each heat flux are listed in Table 5. The points highlighted in yellow are where the data should cross the heat flux curves, signifying a burn. Next, it was found that a technique to merge the five new curves to ensure a burn should be determined.

	New S&C for 5 kW/m ²	New S&C for 10 kW/m ²	New S&C for 15 kW/m ²	New S&C for 20 kW/m ²	New S&C for 25 kW/m ²
0					
1	14.69	20.16	24.38	29.55	33.90
2	17.36	23.11	27.63	33.79	38.63
3	19.31	25.45	30.23	37.25	42.39
4	20.99	27.42	32.50	40.35	45.57
5	22.32	29.14	34.50	42.95	48.22
6	23.85	30.97	36.56	45.65	50.98
7	24.75	32.25	38.07	47.73	53.03
8	25.93	33.75	39.75	50.11	55.34
9	27.05	35.20	41.48	52.33	57.45
10	28.01	36.51	43.03	54.42	59.31
11	28.99	37.83	44.58	56.36	61.34
12	29.87	39.08	46.02	58.40	63.08
13	30.88	40.40	47.57	60.31	65.15
14	31.79	41.69	48.99	62.37	66.94
15	32.85	43.15	50.70	64.53	68.96
16	33.45	44.13	51.83	66.12	70.43
17	34.33	45.29	53.33	68.10	72.35
18	35.27	46.54	54.81	70.21	74.14
19	35.87	47.66	56.16	72.02	75.88
20	36.79	48.84	57.68	74.11	77.73
25	40.65	54.70	64.94	84.50	86.86
30	44.43	60.46	72.39	95.38	96.25

Table 5: New Curve Derived Points

At no time did the temperature for the 5 kW/m² cross this new curve. So the last point for this heat flux as well as other points of interest (the points highlighted in yellow) were graphed. With these five points plotted, a logarithmic trend curve was calculated producing the equation:

$$y = -7.2215 \cdot \ln(x) + 67.55 \quad (11)$$

This curve, as seen in the Figure 26, intersects with all the points of interest. The new curve is very different from the Stoll and Chianta curve. This is due in part to the way the data for the epoxy-glass sensors changes with changes in heat flux. The data changes sharply within the first 10 seconds and then levels off. The increase in thermal insult is registered immediately, unlike the copper slug sensor data where the increase is noticed towards the end of the exposure. Because of this, the curve has to start at a higher temperature change to register a burn accurately at high heat fluxes, but must decrease to register burns at lower heat fluxes. The Stoll and Chianta has a positive rise because the copper slug sensors register a uniform initial change in temperature (first 5 seconds) for a wide range of heat fluxes and then increase in slope as appropriate to the heat flux present.

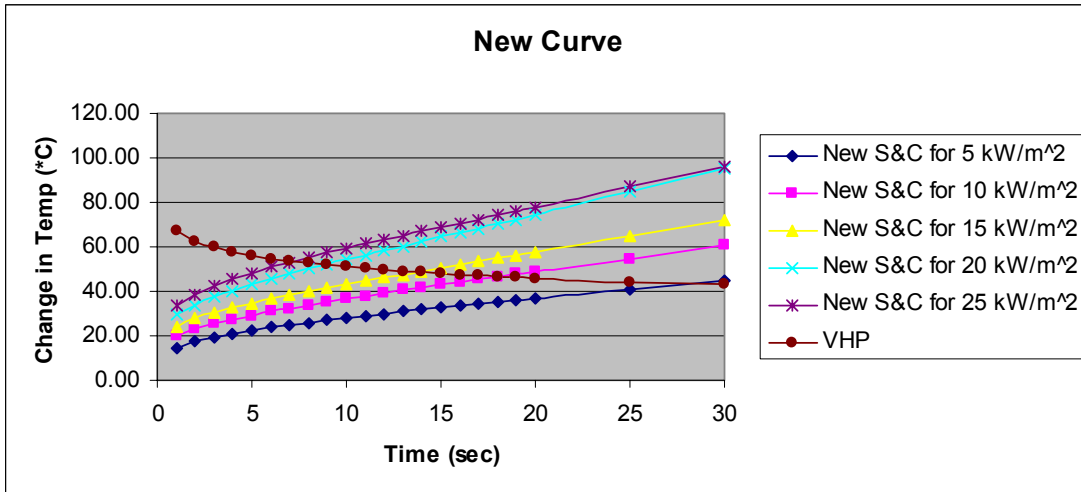


Figure 26: VHP Curve vs. Derived Curves

The new curve was given the name VHP after the members of this project.

4.2 Full Scale Testing Analysis

The results of the full-scale tests conducted at the Fire Lab in Holden showed that an overall cooling effect occurred when the undershirt was saturated. Figure 27 below is the average of all the dry tests, including those conducted for the Navy, versus the average of the five wet tests conducted.

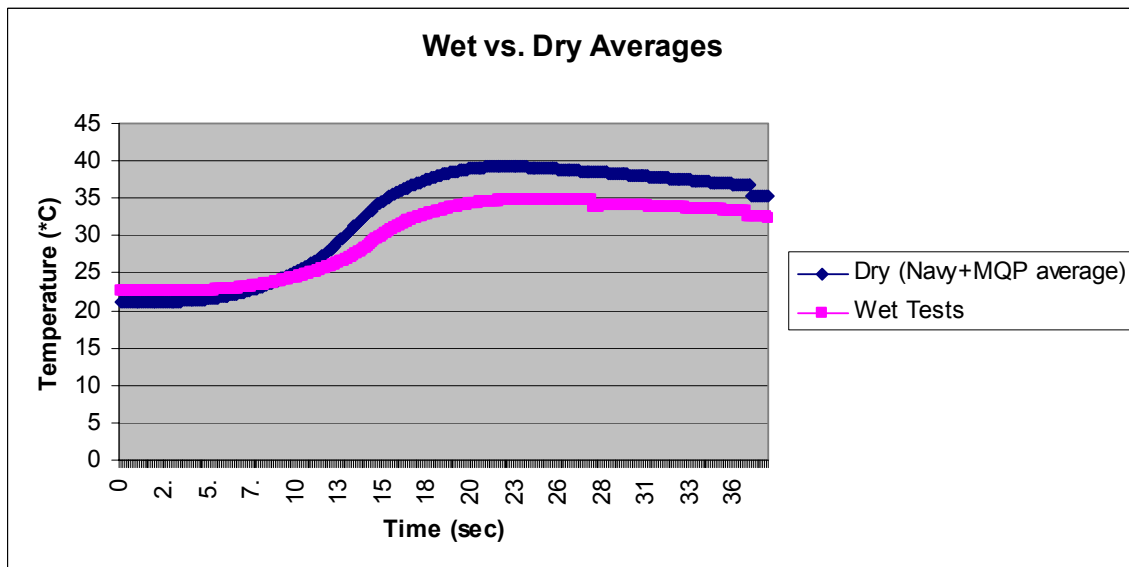


Figure 27: Wet versus Dry Test Averages

With the full-scale test, a major source of error took place when modifying the data to analyze with the VHP curve. The VHP curve is based off the change in temperature from an initial starting temperature (ideally room temperature). This temperature is the temperature right before the sensor is exposed to the heat insult. For the full-scale tests, this would be when the manikin is at the opening to the room (approximately 14 seconds from the start of data acquisition). Using a plywood barrier, it was attempted to block the radiation from insulting the sensors before the manikin reached the opening. As can be seen from the data, there was marginal success for the sensors were exposed to some radiation near the door. Because of this, the temperature change data lines are not as accurate as possible since the initial temperature is already higher than room temperature.

Figure 28 presents the data from the three dry tests run solely for this project. From this graph, it can be seen that there were few sensors exposed to temperatures that would result in a second degree burn (temperatures higher than 55°C). The highest curve represents the sensor located in the mouth that was left exposed, and explains the +100°C reading.

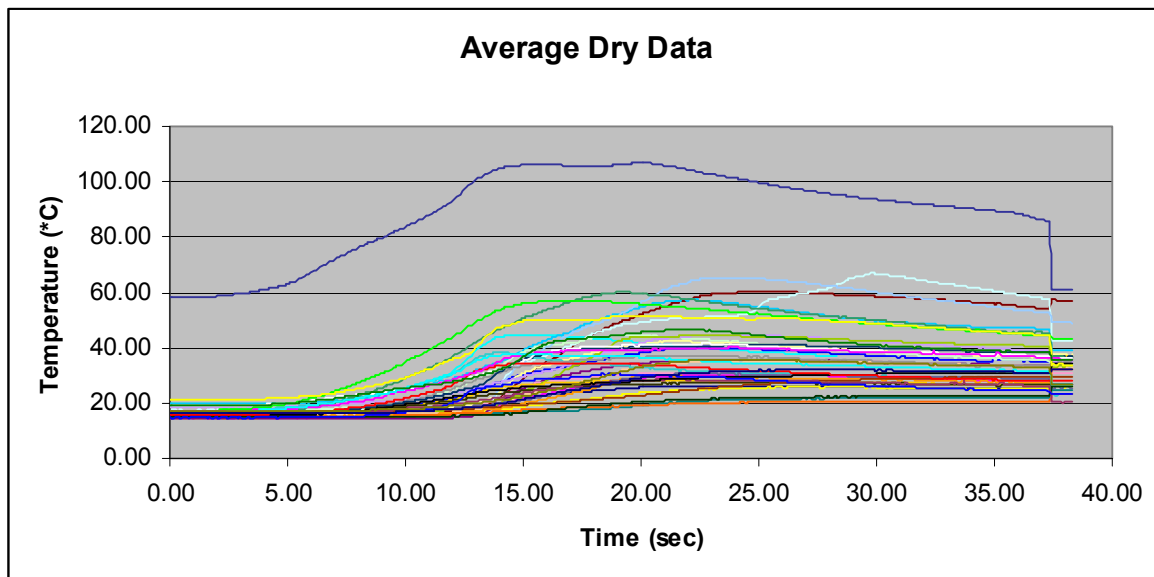


Figure 28: Full Scale Dry Temperatures Averages

Although from this graph it may seem likely that a few burns would occur, from analysis done with the VHP curve and initial temperature starting at 14 seconds, only one

burn was definitely determined. The two closest lines may be assumed to be burns since the inaccuracy of the curve is based on the varied readings of the epoxy-glass composite sensors.

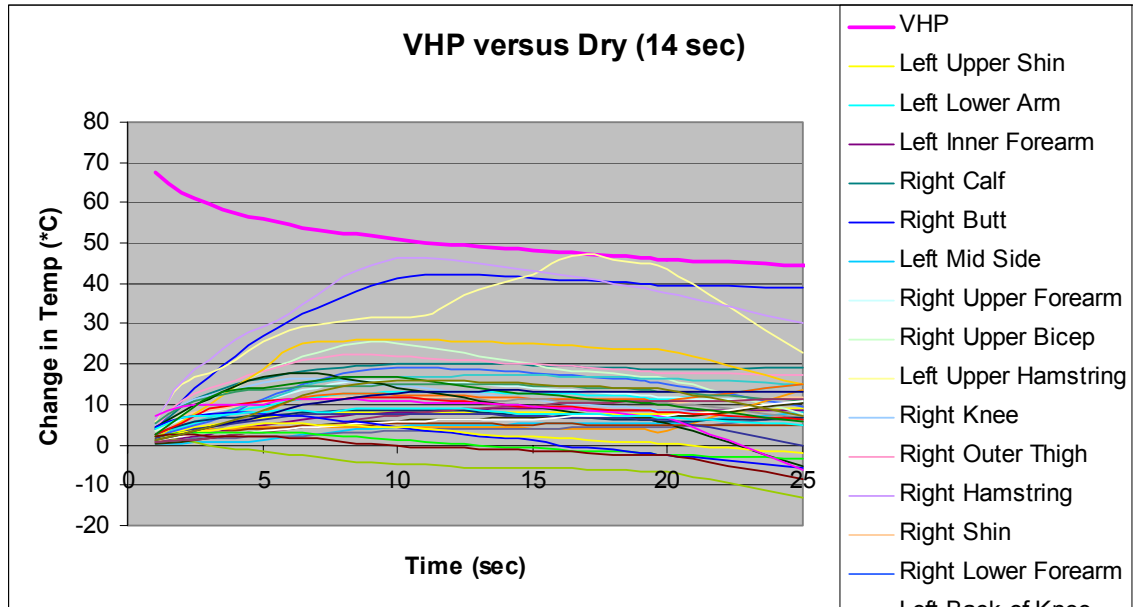


Figure 29: VHP vs. Dry Temperature Averages (14 sec)

When the data curves were skewed to have the initial value taken at 10 seconds, in order for the initial temperature to be closer to room temperature, the following analysis was found. Now, two sensors definitely show burns and, again, one is close enough to be an assumed burn, given the estimated nature of the VHP curve.

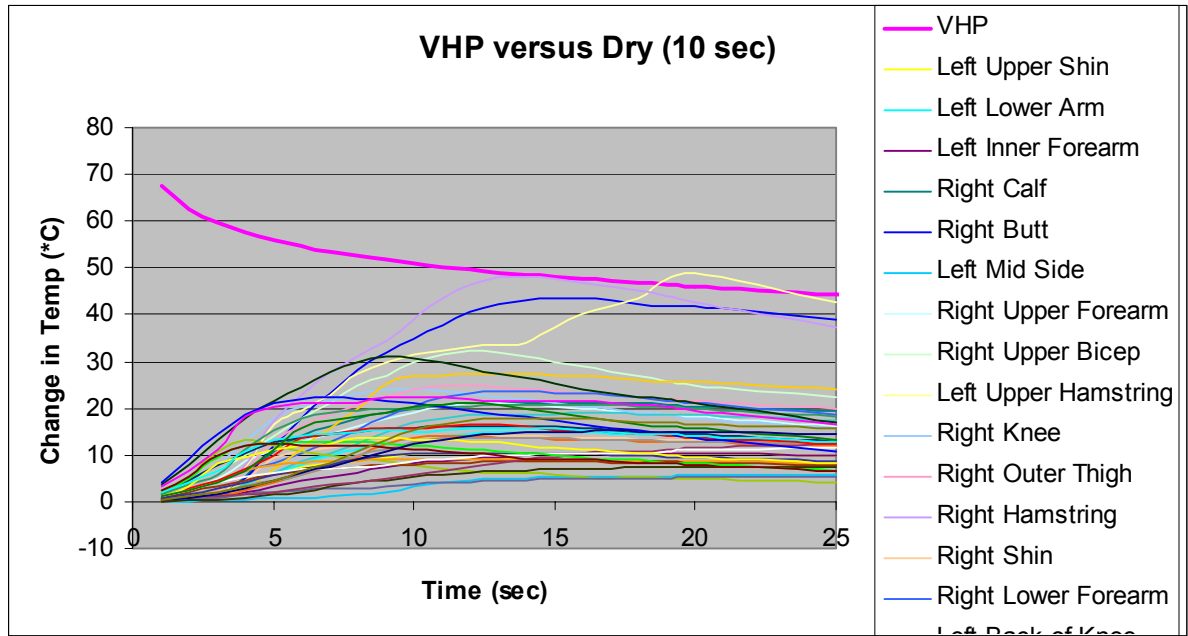


Figure 30: VHP vs. Dry Temperature Averages (10 sec)

Table 6: High Temp vs VHP Burns (Dry) compares the three burns, the three next closest as found by the VHP curve, and the sensors that reached a temperature of 55°C.

High Temperatures	VHP
Dry	Dry
mouth (105 °C)	left upper hamstring
left upper hamstring (65 °C)	right hamstring
right hamstring (65 °C)	right butt
right butt (60 °C)	right upper bicep
right upper chest (thermocouple) (60 °C)	right upper chest (thermocouple)
left thigh (58 °C)	right elbow
groin (50 °C)	

Table 6: High Temp vs VHP Burns (Dry)

There is a relative consistency between the high temperatures and burns. The mouth did not register as a burn because its initial temperature was close to its maximum due to the fact that it was an exposed sensor. As seen for covered sensors in the cone testing, the sensor will have a dramatic increase in temperature when exposed to a heat flux. Since the curve is based off of the sensor being covered by clothing, and with the expected outcome of a large increase in temperature, both of which the mouth did not meet. It was uncovered and already near its steady state temperature for the given heat

flux when the manikin reached the door. Therefore, no significant rise in temperature was recorded and no burn established. The curve is not appropriate to analyze any data if the two layers of clothing used for these specific tests are present.

The same steps were taken to analyze the wet data. Comparing the dry data with the wet data, it was found that the wet tests resulted in lower temperatures. The highest temperature reached with the wet undergarment was 50°C which is much less compared with the 65°C reached during the dry test.

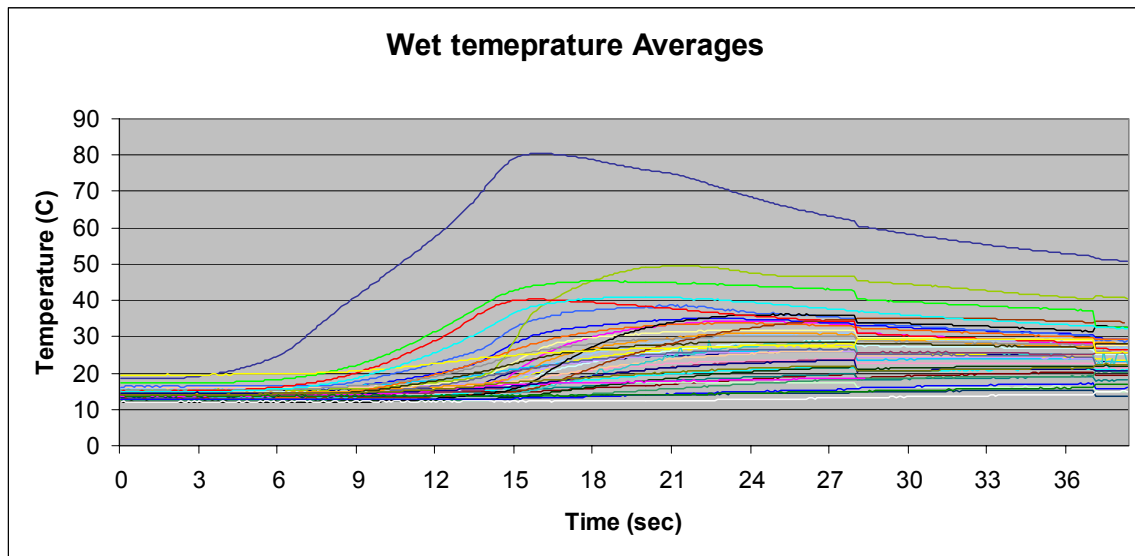


Figure 31: Full Scale Wet Temperature Results

Even with the cooling that occurred during the wet tests, a few sensors recorded a second degree burn with temperatures exceeding 55°C. When analyzed with the VHP curve taking 14 seconds as the start time, none of the sensors intersected the curve and therefore, by this method, no second degree burns were reached. Compared with the dry data, the wet data does not reach the closest data line by only coming within 20 degrees of the curve.

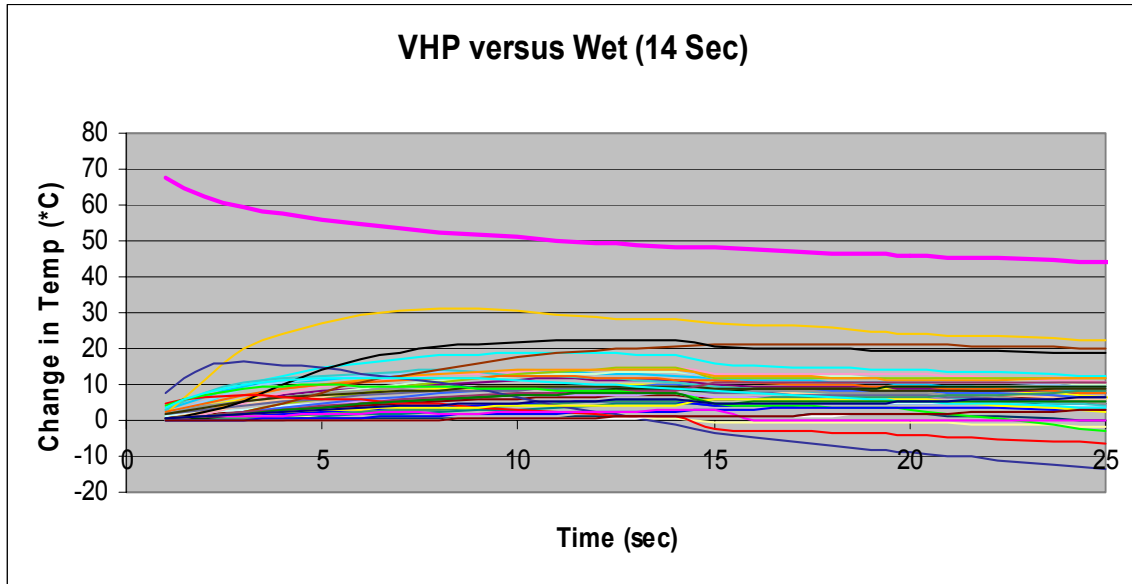


Figure 32: VHP vs. Wet Temperature Averages (14 sec)

With the start time at 10 seconds, to more closely resemble room temperature, the difference is closed to 15 degrees between the curve and the closest data line. After this analysis, it was determined that for high heat insult for a short exposure time tests, moisture built up under the clothing will help to cool the sensors.

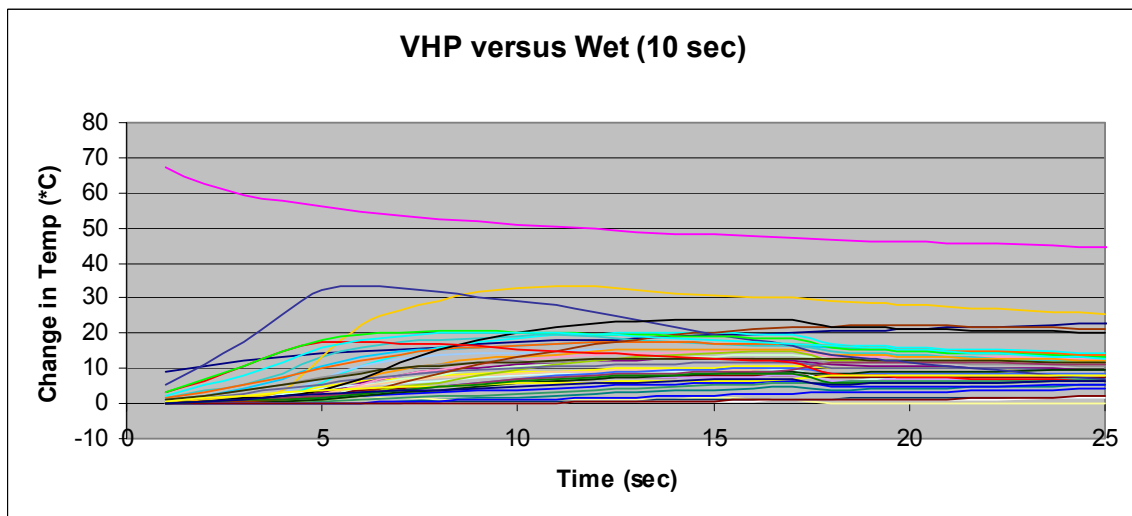


Figure 33: VHP vs. Wet Temperature Averages (10 sec)

When the highest temperature readings for the wet tests were analyzed, one interesting sensor was found. For the wet tests, the right elbow reached an average temperature of 50°C. During the dry tests its average peak was 44°C.

High Temperatures
Wet
mouth (80 °C)
right elbow (50 °C)
left thigh (45 °C)
left upper thigh (40 °C)

Table 7: High Temp (Wet)

This shows that the mechanism is different. The moisture prevents the skin from cooling and results in a burn. The results of all the large scaling testing allowed us to see that the testing procedure used was not appropriate for this research. Next, testing was conducted in the cone calorimeter to test dry and wet fabrics at low heat fluxes over a long period of time. The following are the results from those tests.

4.3 Small-Scale Testing – Cone Calorimeter Series 1

The first set of cone tests were run at 5 kW/m² for 300 seconds. As can be seen in Figure 34, from the time-temperature curves, significant cooling was found. The letter and number designation in the legend was the name given to the sensors to track its specific data. The three sensors chosen for this test (1, 2 and F) all had similar time-temperature curves. Therefore, the results between the sensors are interchangeable and can be compared against each other.

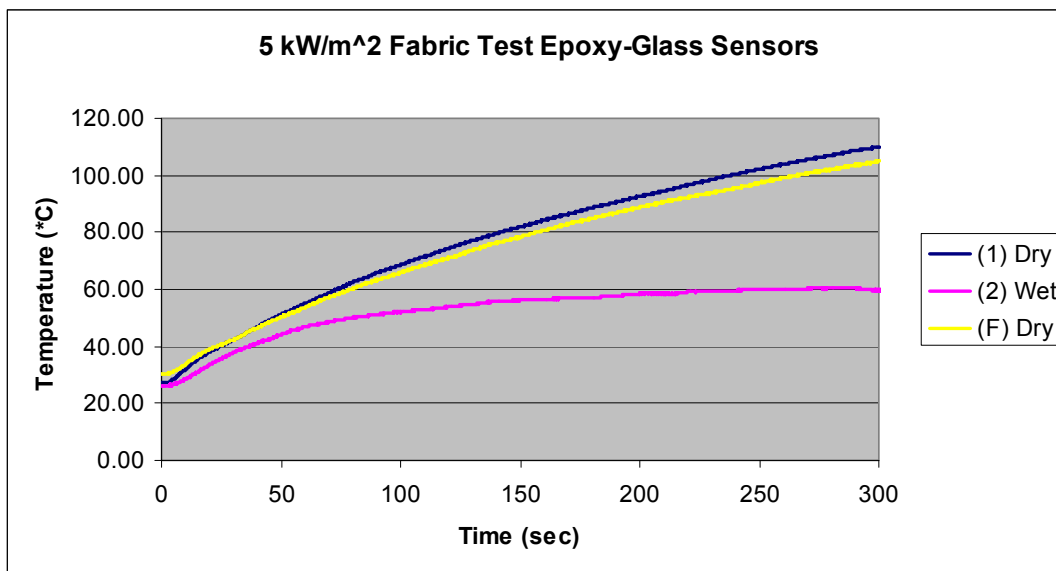


Figure 34: Fabric Cone Test Epoxy-Glass Sensor

The data was also analyzed against the VHP curve to identify places where the wet data may have had a stronger rise in temperature. This was not found, and both the wet and dry data produced similar change in temperature versus time curves.

To mimic the large-scale tests which were run for a short period of time and to mimic the Stoll and Chianta curve which were run for a short period of time (30 seconds), it was attempted to identify a scald burn in only 30 seconds. This can be seen in Figure 35.

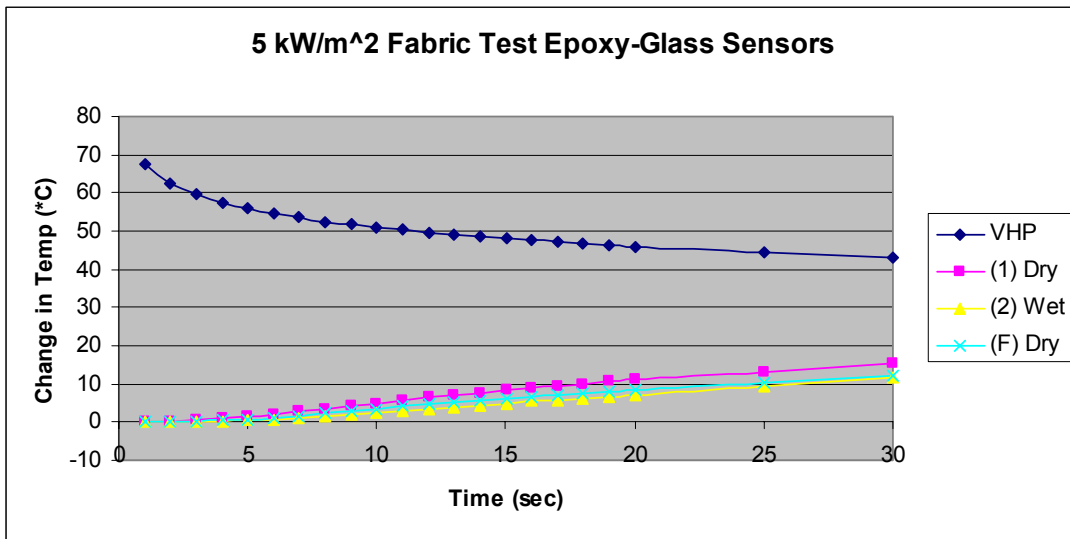


Figure 35: VHP vs. Fabric Cone Testing Epoxy-Glass Sensor

For the first tests, the 5 kW/m² heat flux produced curves that did not intersect with the Stoll and Chianta curve and, therefore, the VHP curve. It was decided to boost the heat flux to 10 kW/m² as it was found earlier that an exposed epoxy-glass sensor will intersect the curve. Therefore, it was hoped the covered sensor would also produce data that intersected the curve. Other motivation to use this heat flux was that the information from the report from the University of Alberta showed results from similar tests with this heat flux. The procedure stated that a 10 kW/m² heat flux for 100 seconds was implemented. These parameters were used with the intention of producing similar results in the cone calorimeter.

Similar results were found with this heat flux and time. Time-temperature curves demonstrated a cooling effect with the wet tests as compared with the dry, as can be seen in Figure 36. However, both sets of data would result in a burn because of the temperatures reached.

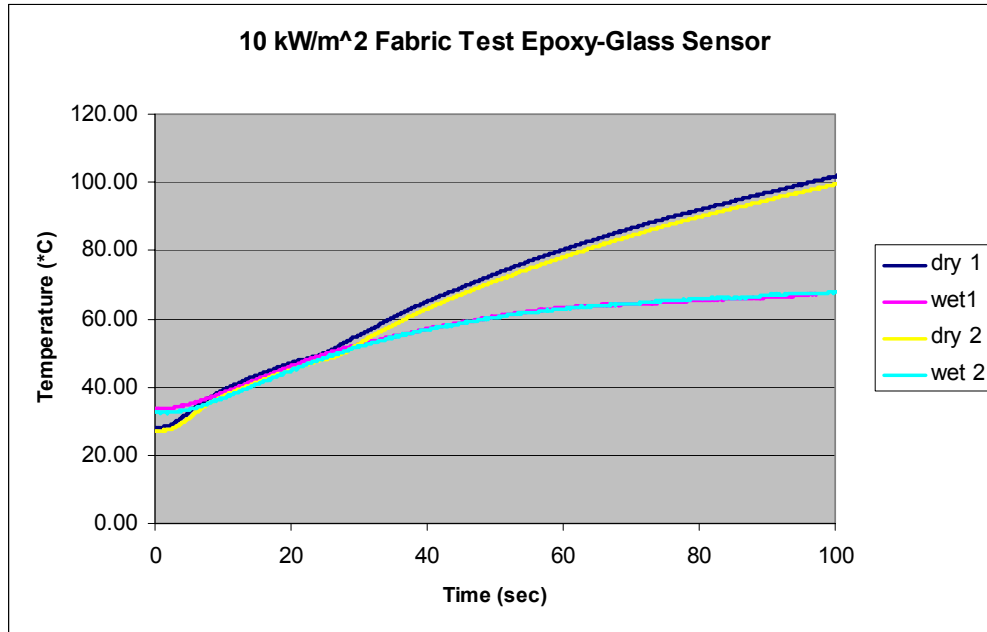


Figure 36: Fabric Cone Testing Epoxy-Glass Sensor

When analyzed against the VHP curve for the higher heat flux, there was a noticeable difference between the wet and dry data. The dry data produced a slightly greater increase in temperature.

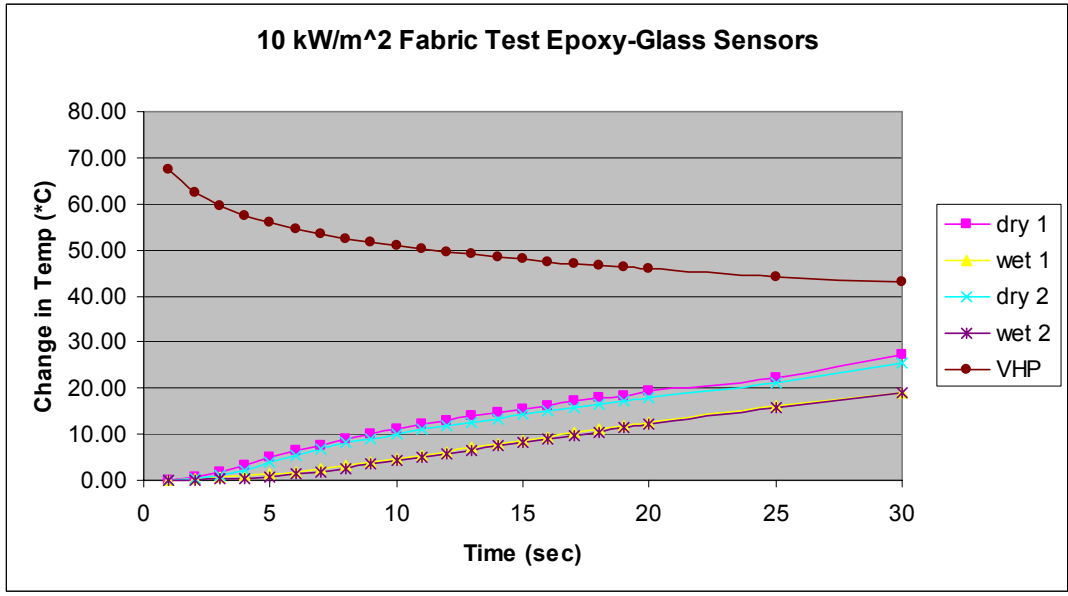


Figure 37: VHP vs. Fabric Cone Testing Epoxy-Glass Sensor

The same test step up was then used for the copper slug sensors to determine if the type of sensor would show any differences. The time-temperature curves produced with the copper slug sensor did not show as significant a cooling effect as the epoxy-glass sensors did. It should be noted that the difference in starting temperature is a result of the sensor not cooling down completely before being used again. Even with the discrepancy in starting temperature, the wet and dry curves are very similar.

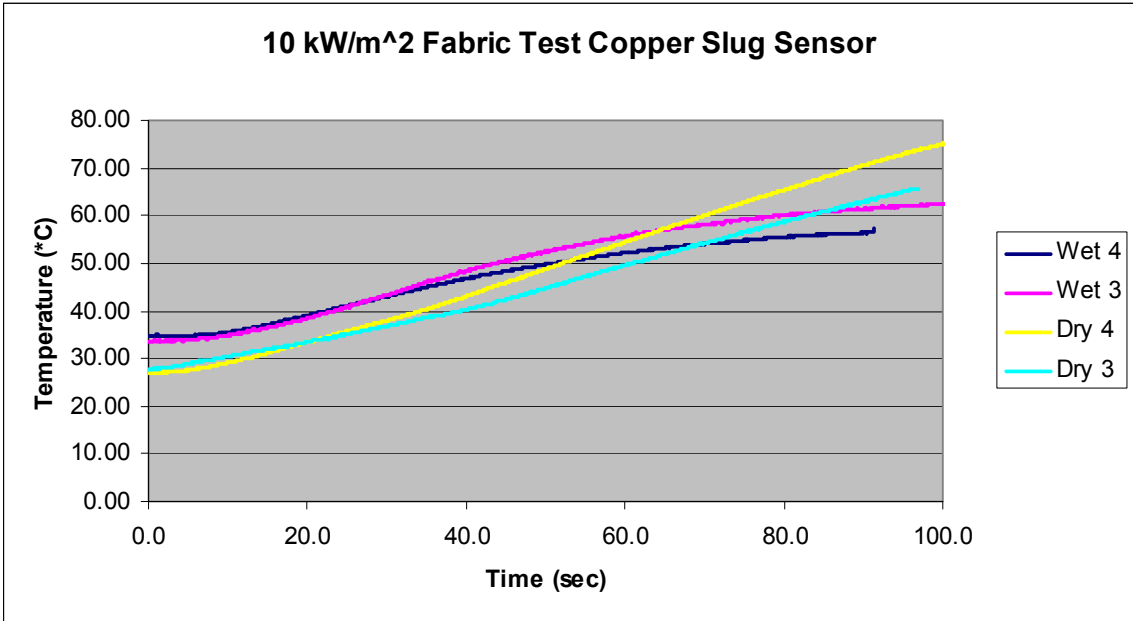


Figure 38: Fabric Cone Testing Copper Slug Sensor

When analyzed with the Stoll and Chianta curve, it was found that all four data lines have a similar slope. At first glance of Figure 39, it may seem as if the wet data is slower to rise than the dry data. However, at 30 seconds, the wet data from copper slug sensor 3 (yellow line) rises above the dry data from the same sensor (maroon line). This could be as a result of the moisture in the fabric vaporizing.

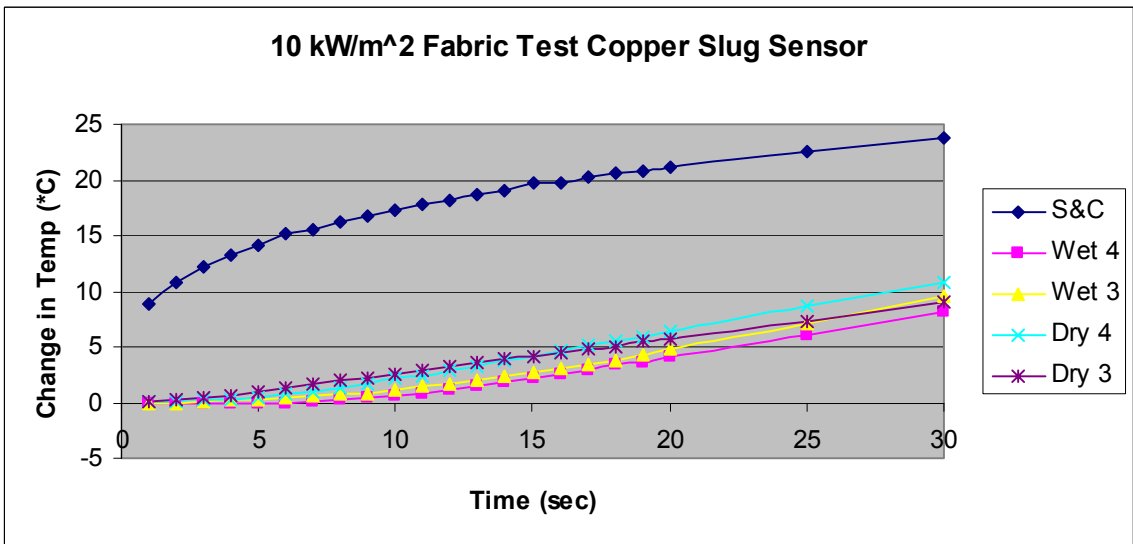


Figure 39: Stoll and Chianta vs. Fabric Cone Testing Copper Slug Sensor

The change in temperature curve was projected out to 90 seconds to see if this change may develop more. It was found that the wet curve extends the gap and has a rise in temperature a few degrees higher than the dry data. The other wet data also comes close to surpassing the dry data.

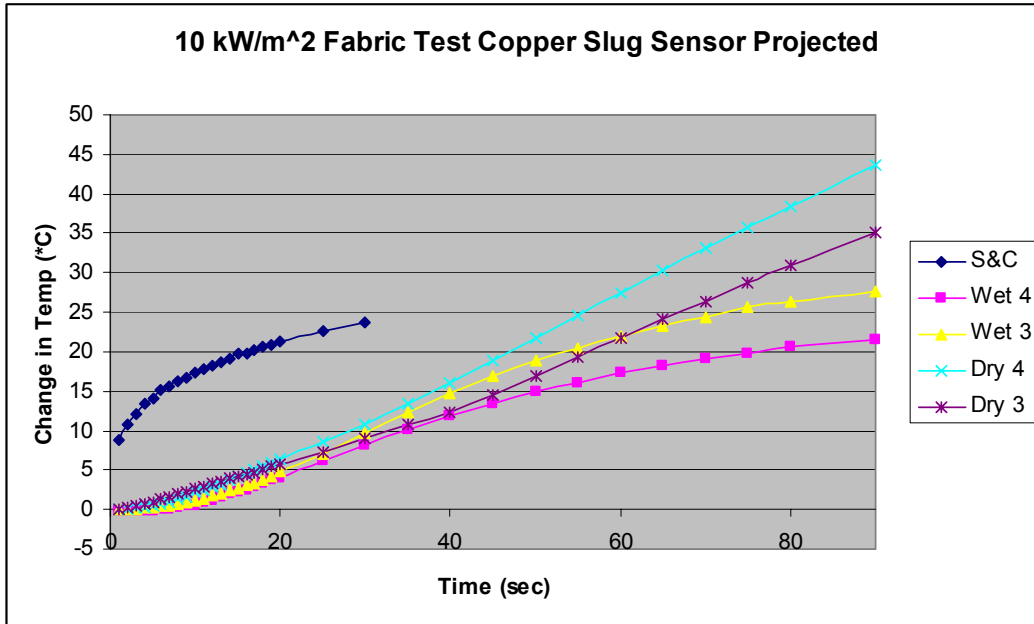


Figure 40: Stoll and Chianta vs. Projected Copper Slug Test

These results show that moisture has an effect on temperature. Figure 38 demonstrates the principles from the equations we developed. The wet temperature is greater around 40 seconds because the water is starting to evaporate and the latent heat of vaporization is increased. The skin is not able to cool down and the heat storage term in the skin increases. (For these tests, the copper slugs were used at heat fluxes of 5 kW/m² and 10 kW/m² for a time an extended period of time (10 minutes or until the sensors reach steady state)).

4.4 Small-Scale Testing - Cone Calorimeter Series 2

4.4.1 Heat Flux and Burn Analysis

Found in Sipe's thesis are Microsoft Excel worksheets that allow the user to input time-temperature data and output graphs of the heat flux present at the surface of the

copper slug. The results produced are independent of any barriers the heat incident had to pass through to reach the sensor.

With the full-scale tests, the size of the fire was unknown and could vary based on the weather on the day of testing. For these tests, we were interested in the heat flux that reached the sensors so the data from the copper slugs were inputted into the worksheets. On a side note, the worksheets are only calibrated for the specific type of copper slugs that were used in these tests and, therefore, the epoxy-glass composite sensor data could not be used.

The following graphs show the heat flux reached by the copper slugs in both the dry and wet full-scale tests. The average time-temperature data for the respective tests was used.

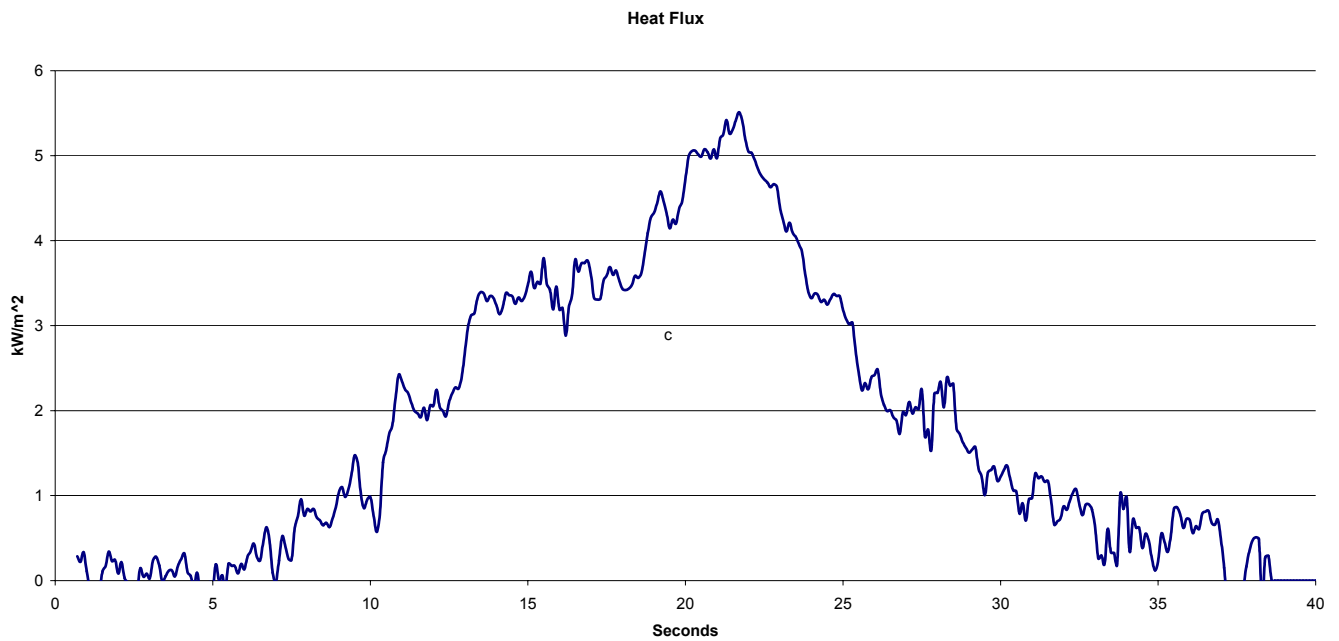


Figure 41: Heat Flux at Sensor - Dry Full Scale

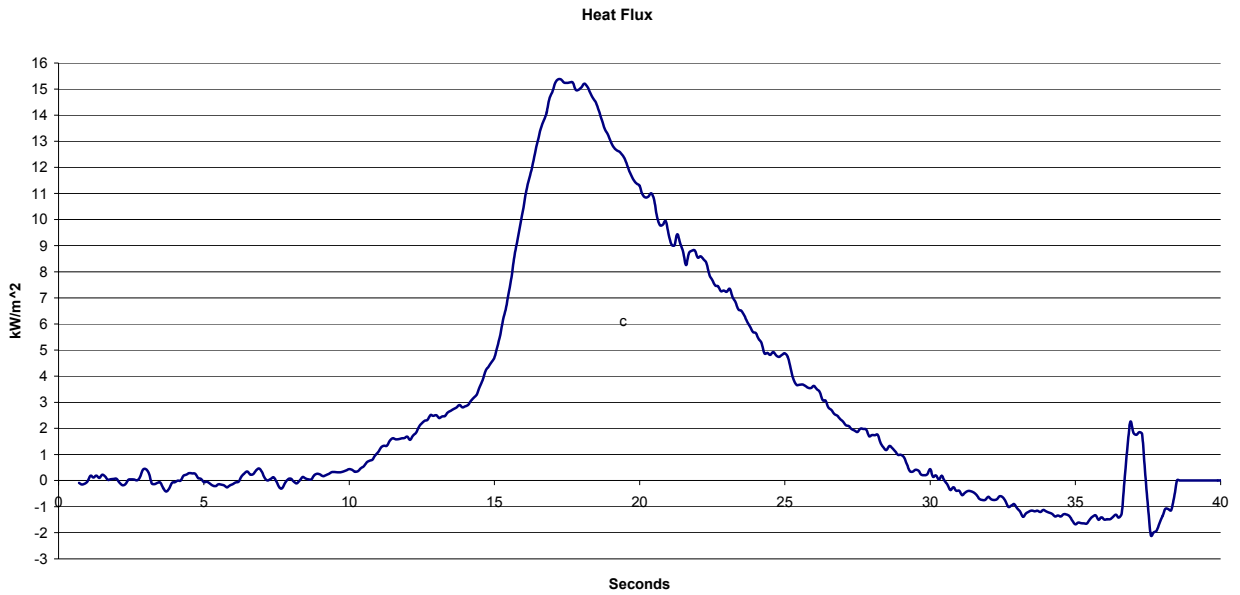


Figure 42: Heat Flux at Sensor - Wet Full Scale

These graphs demonstrate a result different from the previous results seen. The copper slugs in the wet test experienced a heat flux almost three times as much as it had previously experienced when the undershirt was dry. The time-temperature graph in Figure 43 shows that a high temperature was also reached when there was moisture under the suit.

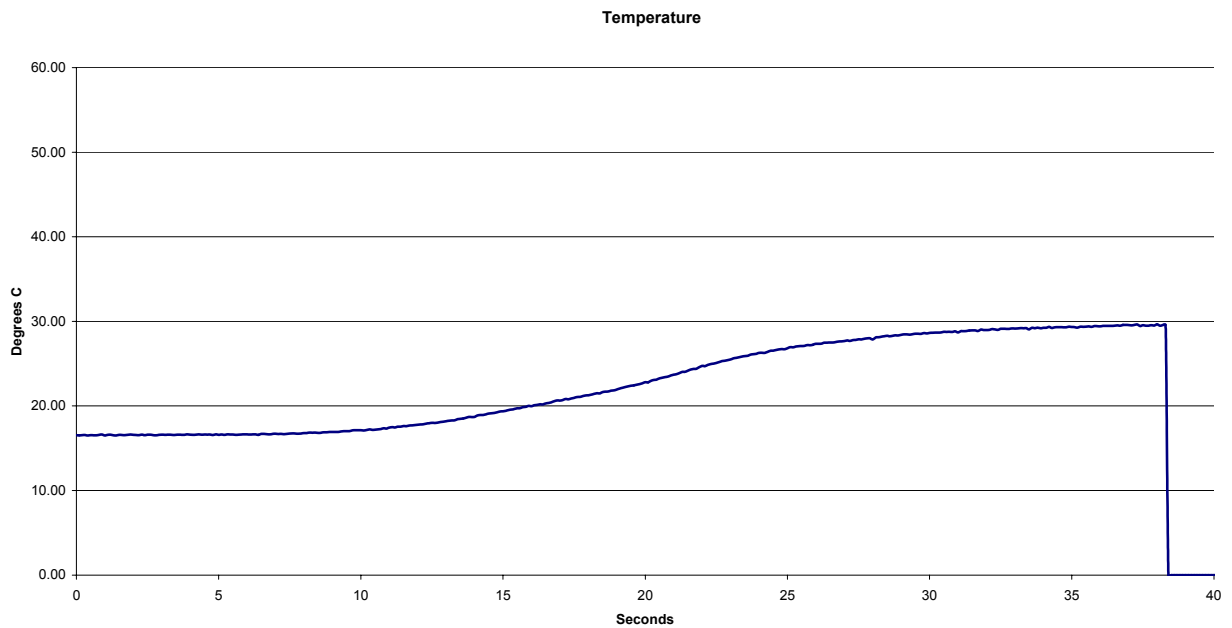


Figure 43: Time-Temperature Dry Full Scale

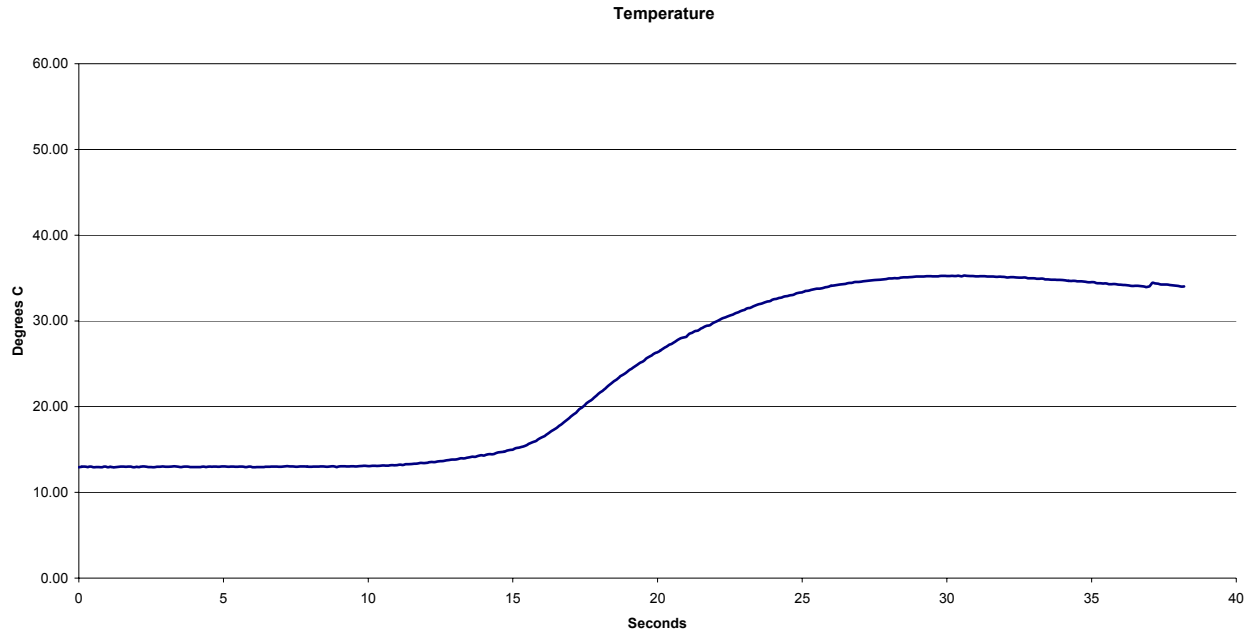


Figure 44: Time Temperature Dry Full Scale

As stated previously, the results thus far confirmed that the tests for cone calorimeter should be run for a longer period of time. Also, under the suggestion of Sipe, data acquisition started a minute before the shutter was opened and the sensor was exposed to the heat flux. For these tests the heat flux was kept at 10 kW/m^2 .

Running tests at longer periods of time with lower heat fluxes allows us to accomplish three reasons. First, raising the temperature of the water in the moisture barrier high enough may allow a scald burn to register. Second, in the rate of condensation equation (equation (10)), the volumetric flow rate term, (\dot{m}_v''') , poses no effect if the moisture barrier is exposed at high temperatures for short periods of time since it will not condense. If this does not happen then there is no volumetric flow rate because there are no buoyant forces that impulse it. Hence, the change in latent heat of vaporization, (Δh_v) , will also be low due to the lack of change of state of the water.

One more factor that has not been discussed is the storage term. As it names states; its stores energy, also termed as heat. Since this term is a temperature derivative with

respect to time, it can be inferred that the longer time the sample is heated, the more storage the sample will have.

These next tests ran for 390 seconds. The time-temperature graphs for the dry and wet tests are shown, respectively, in Figure 45 and Figure 46. The wet time-temperature graph shows an initial jump in temperature when the shutter is opened but then steadies out. After 300 seconds, it again begins to rapidly increase. From this, it can be seen that the moisture stored the heat incident until, it is assumed, the moisture underwent a phase change.

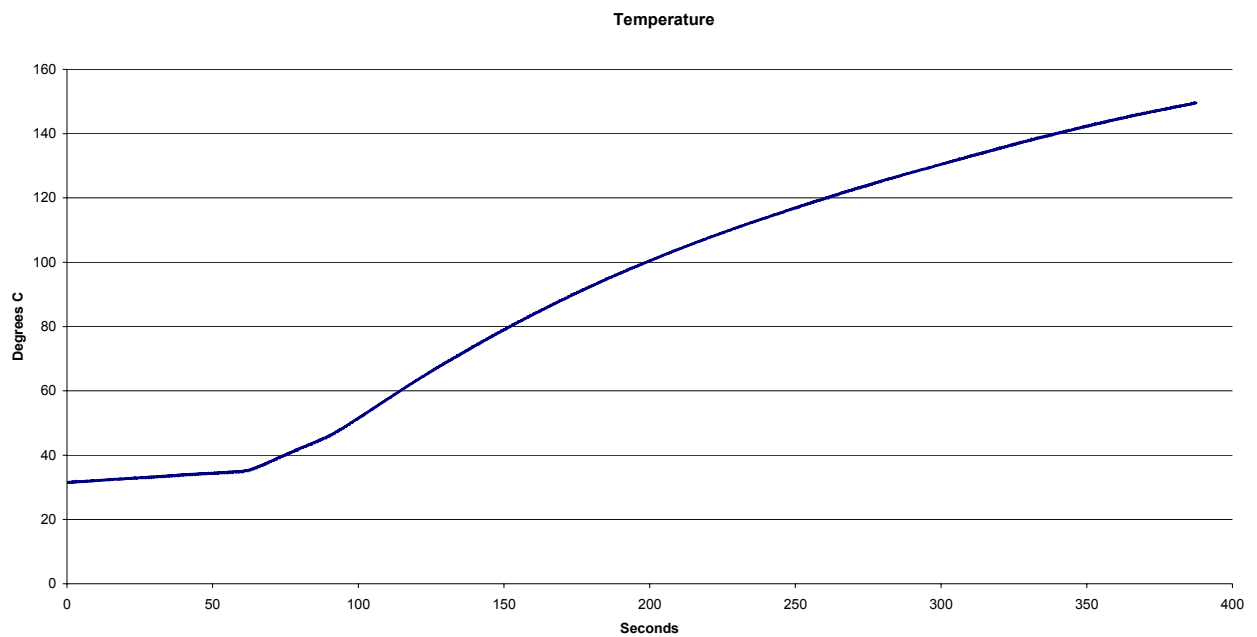


Figure 45: Time Temperature, Dry (390 seconds)

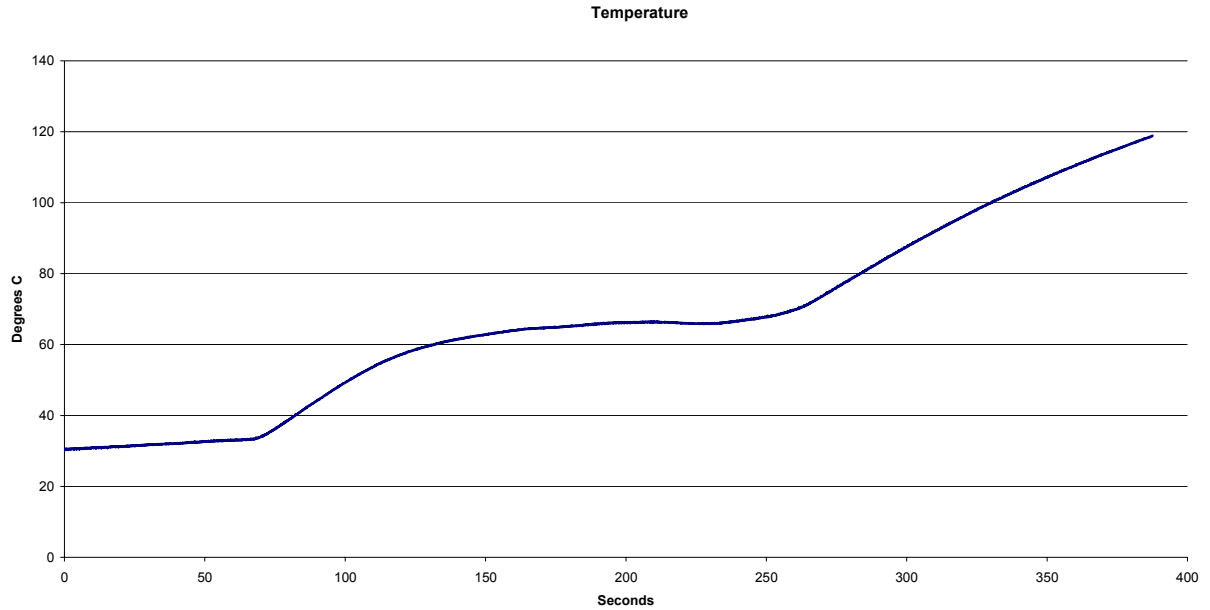


Figure 46: Time Temperature, Wet (390 seconds)

The heat flux graphs support the assumptions as stated above. The heat flux graph for the wet data demonstrates that when the shutter is opened there is a prompt reaction to the sudden heat insult but the moisture then absorbs the heat. Again when the moisture evaporates, the heat flux increases at the sensor similarly as if it were a dry test due to the rate of condensation term, (Equation 10).

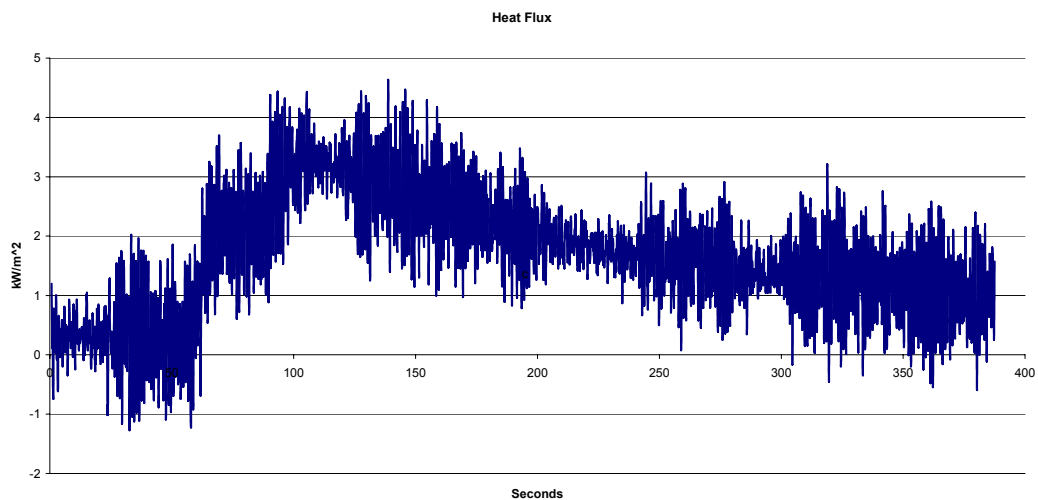


Figure 47: Heat Flux at Sensor, Dry (390 seconds)

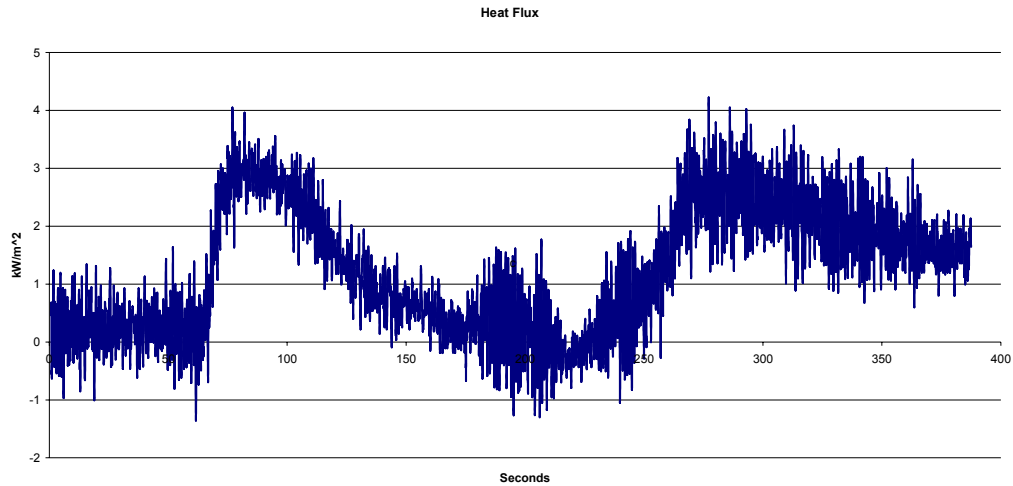


Figure 48: Heat Flux at Sensor, Wet (390 seconds)

With the given data, it is no surprise that a burn occurred quite rapidly for the dry test and was delayed until after the moisture was gone for the wet test (after 300 seconds). Figure 49 and Figure 50 visually depict when burns occur which are based off of Henrique's Burn Integral. For the given data, if the Henrique's Burn Integral is less than 0.53 no burn occurs, if it is 0.53 to 1.0 a first degree burn occurs, and if it is 1.0 or greater a second degree burn occurs. In Figure 49, the yellow line is the first degree burn threshold while the red line is the second degree burn threshold.

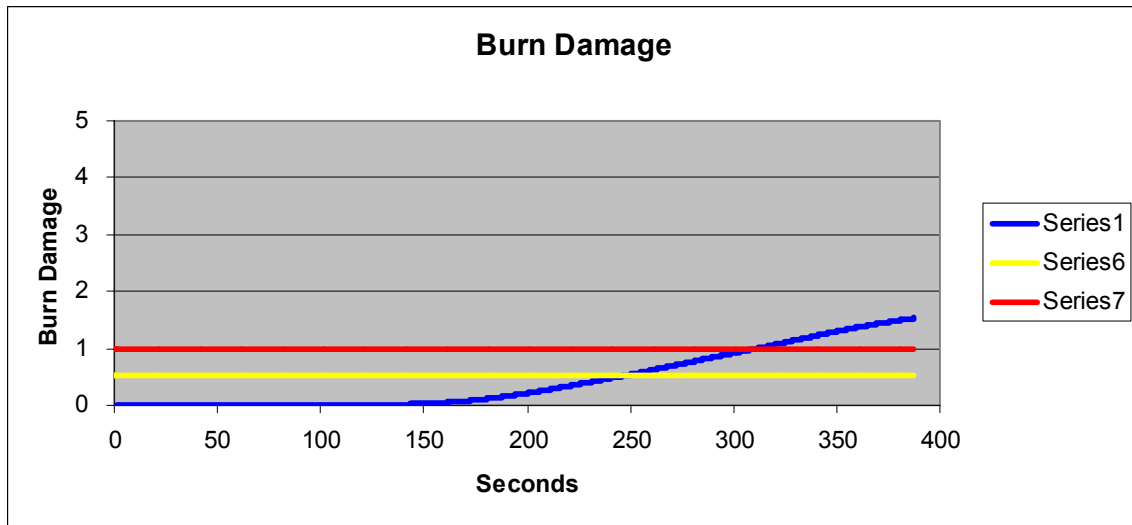


Figure 49: Henrique's Burn Graph, Dry (390 seconds)

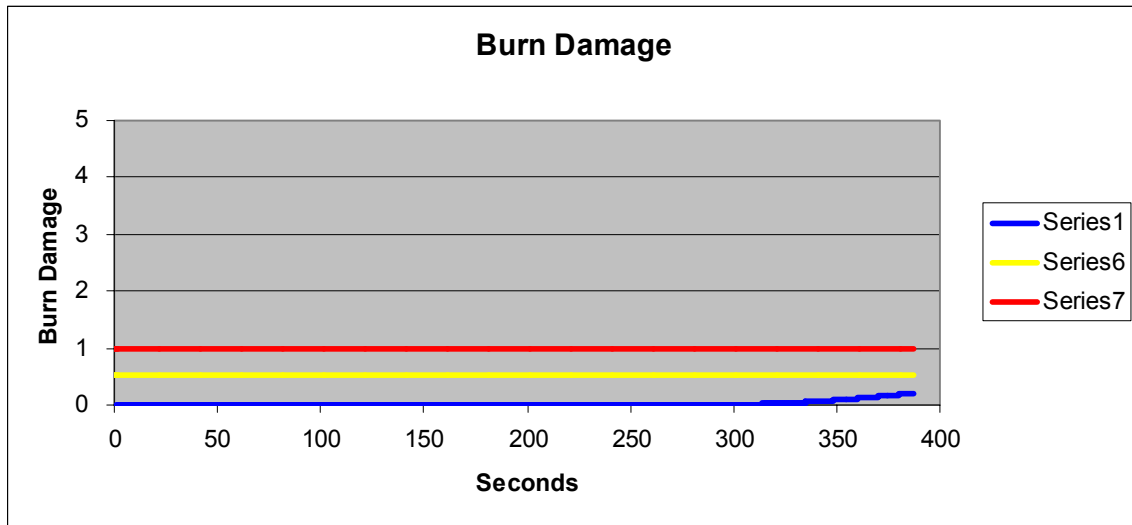


Figure 50: Henrique's Burn Graph, Wet (390 seconds)

In Figure 50, the blue line, representing the Henrique's Burn Integral output for the wet data input, rises towards the thresholds. It is assumed that within the next minute the line would cross the second degree burn threshold which is based on the trend that after 300 seconds the data becomes similar to the dry tests. In attempt to prove this, tests were run for 900 seconds. Unfortunately, the extensively high temperatures reached during this test broke the sensor and only a dry test was completed. Figure 49 through Figure 51 were compared with the 600 seconds tests and as would be expected with a longer test, a burn occurs at a faster rate.

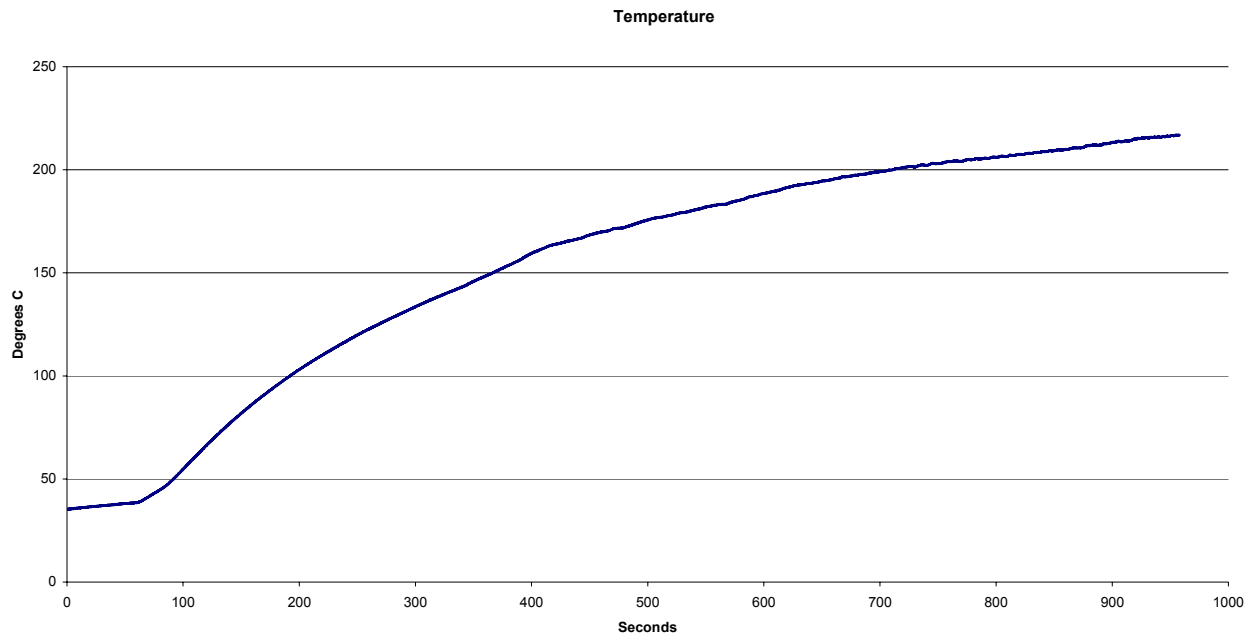


Figure 51: Time Temperature, Dry (900 seconds)

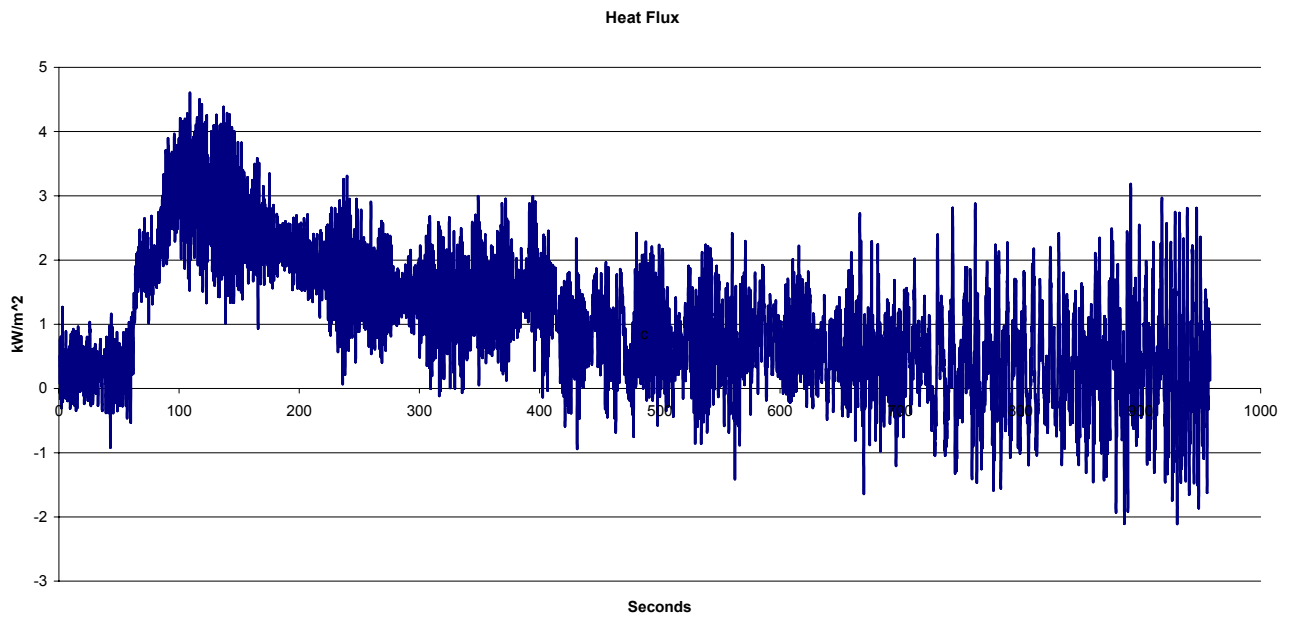


Figure 52: Heat Flux at Sensor, Dry (900 seconds)

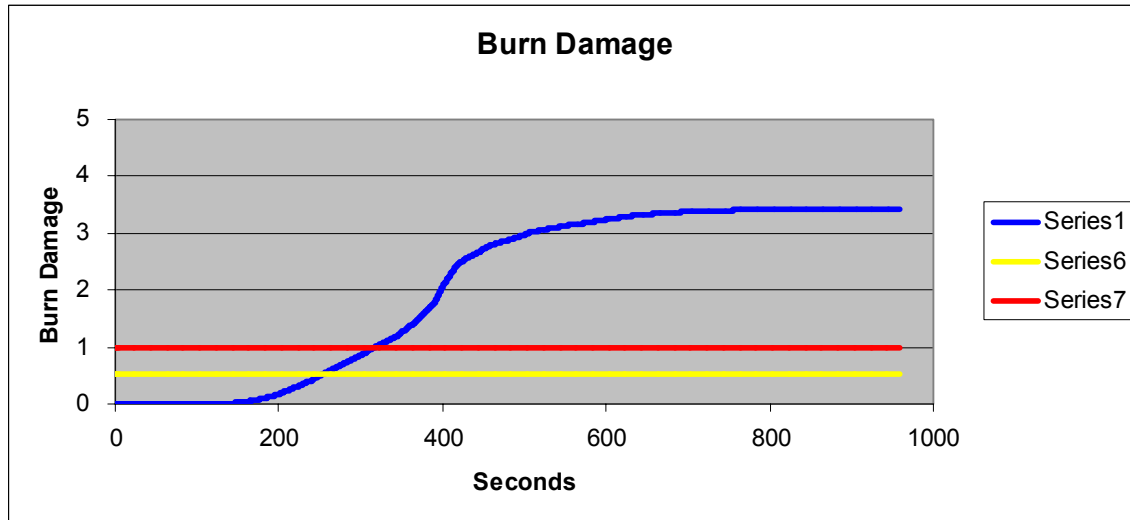


Figure 53: Henrique's Burn Graph, Dry (900 seconds)

From the beginning of testing, it was found that the same methods used to analyze the copper slug sensors could not be used for the epoxy-glass sensors. Bench scale testing was conducted in order to develop a curve that could be used to analyze the data from these sensors. The curve was not very effective and more calibration is needed to produce a more realistic curve.

Both sensors were continued to be used for the small scale testing. From these tests, there were instances in the data where higher temperatures were reached with moisture than dry garments. These instances verified the equations we developed. Although no reproducible data was collected, it was still demonstrated that steam burns do occur and are an issue over dry burns. With better data analysis methods that take into account the moisture barrier, more concrete results will be obtained.

5 Conclusions

The goal of the project was to determine if scald burns could be tested in a lab setting to further facilitate future research with functional guidelines. Research showed that scald burns are not easy to identify nor easy to reproduce due to the complexity involved in the process.

The lack of empirical data on scald burns also compounds the issue. The physics behind a scald burn are much different than a dry heat burn. Moisture is absorbed by materials touching the skin and fill in the air gaps. This increases the thermal conductivity of the material. The moisture layer on the skin also prevents the skin from producing sweat to release heat. Therefore a scald burn can occur at lower temperatures than a dry heat burn. These factors make the current analysis tools for predicting a burn insufficient. Our research has shown that scald burns can be set up in a lab, but empirical data that correlates the transport of heat through moisture to the skin and when a scald burn occurs is needed to analyze the tests.

The lab settings reported were the most reliable for small-scale tests and large-scale tests. If a large-scale test is desired, then it was found that the use of a traversing manikin equipped with sensors should be used. The number of sensors that the manikin comprises is wholly dependant on the data acquisitioning capacity of the lab. It should however be noted that if considerably fewer sensors that spots in the manikin are employed, personal criteria should be placed upon the location of the sensors depending on the desired results. The large-scale testing facility used for this project was the Fire Lab in Holden, Massachusetts.

For the small-scale testing it was found that using the cone calorimeter was the best option. The cone calorimeter that was used for this project was the one located in the WPI Fire lab. When using the cone calorimeter, samples of 0.11 m by 0.11 m cloth were layered as the clothing was in the large-scale tests. Different heat fluxes were used in the cone calorimeter in order to mimic data found in a report of the University of Alberta. The varying heat fluxes also allowed us to identify the appropriate temperatures at which

burns occur. The setup in the cone calorimeter that mimicked burns the best was using a 10 kW/m^2 heat flux over an extended period of time of 900 seconds (15 min.). Even though a second-degree burn was technically not achieved, the curve perfectly followed the trend. It is important to re-state that the reason why these tests could not be conducted for longer periods of time is due to the fact that the sensor reached 200°C and broke.

However 200°C is a temperature big enough to reach burns of fifth or sixth degree in the skin; but the data output barely registered a second degree burn. This discrepancy between the temperatures registered by the sensor and the calculated data shows that the underlying process used to compute the registered temperature is misleading. The reason for the recorded inconsistency deals with the fact that the equations used to calculate the degree of burn *do not* take in account the effect of the moisture barrier. Among the effects that the moisture barrier causes, it prevents the skin from sweating and as a result it can't cool down from the thermal insults received. So the accuracy of the calculation is very debatable due to this fact.

The test procedures created in this project showed signs of progress in predicting scald burns. The procedure we used allowed for consistent data to be obtained. Again if a method for analysis was available, that accounted for a moisture layer at the skin and took into account the physics previously stated, then we would have found more accurate burns. The described method used to wet the undergarments in the methodology chapter was highly accurate in moistening the fabrics uniformly with the same amount of water. This is extremely important as it allowed for reproducible results.

Different types of sensors were also used in order to determine which data acquisition method is better. It was found that unless a method and specific properties are provided to linearize the data coming from the epoxy-glass composite sensors supplied by the Navy, they cannot be used. The epoxy-glass composite sensors proved to be highly unreliable and therefore using copper slugs would be a much safer option. Many difficulties were encountered when analysis was required for the epoxy-glass composite sensors due to the lack of information and interest given from the Navy. On

the other hand, the copper slugs that were also used belonged to a past WPI M.S. Thesis created by Joel Sipe. Thus, all the information needed to estimate burns with the copper slugs, its properties, and even spreadsheets for the finite differential method were readily available.

6 Recommendations

The recommendations discussed in this chapter were purely developed after observations were made to the empirical data and procedures throughout the experimentation.

- Additional research should be done regarding the transport of fluids in porous media to improve the existing governing equations. The existing governing equations work well under the assumption of having bare skin exposed to a thermal insult. However, the focus of the project was to research scald burns and not just bare skin burns. The presence of the moisture barrier in scald burns produced a great deviation when analyzing results. This can be noted when 200°C were registered at the sensor, but the data only correlated that temperature to a first degree burn.
- For further experiments, if the same epoxy-glass composite sensors provided by the Navy are used, more information will be needed about them. After conducting testing, it was brought to our attention that the sensors should undergo a rigorous calibration procedure. Removing outlier sensors from the group would increase the accuracy of the testing and possibly mimic more accurately the fundamental principles of a scald burn. A proper analysis for these sensors could not be conducted because of the lack of disclosed information from the Navy.
- Even though scald burns were registered in the full-scale test, it is recommended to test with lower heat fluxes and longer time exposures. Due to the underlying physics of scald burns, this recommendation would have *the desired* effect over the skin, as explained with the rate of condensation term. If greater heat fluxes are applied at small periods of time, then the water does not have enough time to go through a phase change, thus defeating the purpose of trying to mimic scald burns.

References

- American Burn Association. "Resources." Accessed: 9 April 2007. Available: http://www.ameriburn.org/resources_factsheet.php
- AMA Atlas. "Skin." 12 Oct 2005. Accessed: 25 Sept 2006. Available: <http://www.ama-assn.org/ama/pub/category/7176.html>
- American Institute for Preventive Medicine. "First Aid for Burns." Health World Online: 1996. Available: <http://www.healthy.net/scr/article.asp?Id=1782>
- Ahrenholtz, D.H., Clayton, M.C., Solem, L.D. "Burns and Wound Management". *Otolaryngologist Clinics of North America* 28:5 (1995).
- ASTM, ASTM F1930: Standard test Method for Evaluation of Flame resistant Clothing for protection against Flash Fire Stimulation Using an Instrumented Mannequin, West Conshohocken: American Society for Testing and Materials, 2007
- Barker, R.L., C. Guerth-Schacher, R. V. Grimes, and H. Hamouda. "Effects of Moisture on the Thermal Protective Performance of Firefighter Protective Clothing in Low-level Radiant Heat Exposures." *Textile Research Journal*, Jan 2006; 76: 27 - 31.
- Barker, Roger L., Barbara J. Scruggs and Chureerat Prahsarn. The International Fire Fighter Protective Clothing Breathability Research Project. Massachusetts: National Fire Protection Research Foundation, 1998
- Barter, Melissa, David Hartman, Jonathan Martin, Aaron Vanney, Jason Kramarczyk and Marc Moseley. "An Improved Mannequin Test", Major Qualifying Project, Worcester Polytechnic Institute, 2004.
- Behnke, W. P., Geshury, A. J., and Barker, R. L., "Thermo-Man® and Thermo-Leg: Large Scale Test Methods for Evaluating Thermal Protective Performance", Performance of Protective Clothing: Fourth Volume, ASTM STP 1133, American Society for Testing and Materials, West Conshohocken, PA, pgs 266-280, 1992.
- Beyler, Craig L ... [et al]. "Predicting 1ST and 2ND Degree Skin Burns From Thermal Radiation". SFPE, 2000.
- BBC. "Science & Nature: The Human Body." BBC: 2005. Accessed: 9 Apr 2007. Available: www.bbc.co.uk/science/humanbody/body/factfiles/skin/skin.shtml

Burn Survivors throughout the World. "Degree of Burns." Sept 2006. Available:
<http://www.burnsurvivorsttw.org/burns/degree.html>

Cankar, Michael. "The Finnish Sauna: What about a bath." Sept 2002. Accessed: 28
 March 2007. Available: <http://www.cankar.org/sauna/health/evaporation.html>

Cavanagh, Jane M., Clothing Flammability and Skin Burn Injury In Normal and Micro-Gravity. M.S. Thesis, Worcester Polytechnic Institute, 2004.

Children's Hospital of Philadelphia. "Your child's Health." Aug 2006. Available:
http://www.chop.edu/consumer/your_child/condition_section_index.jsp?id=-8325

DeCristofano, Barry S. and Landa C. Hoke. Computer Modeling for Individual Thermal Protection. U.S. Army Soldier Systems Command Natick Research, Development and Engineering Center. Massachusetts: March 1997, p 1-49. Available:
<http://stinet.dtic.mil/cgi-bin/GetTRDoc?AD=A324357&Location=U2&doc=GetTRDoc.pdf>

E. I. du Pont de Nemours and Company. DuPont. 2006. Available:
<http://www.dupont.com/>

FEMA, Firefighter Fatalities in the United States in 2001, US Fire Administration, August 2002.

Globe Holding Company, LLC. Globe Firefighter Suits. Sept 2006. Available:
<http://www.globefiresuits.com/>

Kimball, Brian R., Barry DeCristofano and Gerald Caldarella. Thermistor Calibration Procedure for Simulated Skin Sensors. U.S. Army Soldier Systems Command Natick Research, Development and Engineering Center. Massachusetts: March 1993, Available: <http://stinet.dtic.mil/cgi-bin/GetTRDoc?AD=ADA294353&Location=U2&doc=GetTRDoc.pdf>

Lawson, J. Randall. Fire Fighter's Protective Clothing and Thermal Environments of Structural Fire Fighting. Gaithersburg: National Institute of Standards and Technology, 1996.

Lawson, J. Randall. Thermal Performance and Limitations of Bunker Gear. Pen Well: Fire Engineering, Aug 1998.

"Wire Color Codes and Limits of Error" Omega Engineering, Inc.: 2006. Available:
<http://www.omega.com/techref/colorcodes.html>

- Prasad, Kuldeep, William Twilley and J. Randall Lawson. Thermal Performance of Fire Fighters' Protective Clothing. 1. Numerical Study of Transient Heat and Water Vapor Transfer. Maryland: National Institute of Standards and Technology, Aug. 2002.
- Purser, D.A. "Toxicity Assessment of Combustion Products" in "The SFPE Handbook of Fire Protection Engineering", 2nd Edition. National Fire Protection Association, Quincy, Massachusetts, 1995
- Revis, Jr, MD, Don R., "Skin, Anatomy." 17 Feb 2006. Available: <http://www.emedicine.com/Plastic/topic389.htm>
- Sipe, Joel Edwards. Development of an Instrumented Dynamic Mannequin Test to Rate the Thermal Protection Provided by Protective Clothing. M.S. Thesis, Worcester Polytechnic Institute, 2004.
- Stoll, Alice. M. and Chianta, M. A., "Heat Transfer through Fabrics as Related to Thermal Injury", Transactions of the New York Academy of Sciences, Vol. 33, pgs 649-669, 1971.
- Stoll, A.M. and M.A.Chianta, "Burn Production and Prevention in Convective and Radiant Heat Transfer", Aerospace Medicine, Vol.39, No.10, Oct 1968.
- Stoll, A.M. and M.A.Chianta, "Method and Rating System for Evaluation of Thermal Protection", Aerospace Medicine, Vol.40, No.11, Nov 1969.
- Torvie, David, and George Hadjisophocieous. "Research Needs in Protective Clothing for Fire Fighters." Canada: Institute for Research in Canada, 1997.
- T-PACC. Evaluating the Effects of Moisture on the Thermal Protective Performance of Firefighter Protective Clothing in Low Level Heat Exposures. NC State University: 2001.
- Veghte, James H. Design Criteria For Fire Fighters Protective Clothing. Ohio: Janesville Apparel, 1981.
- WPI, "Fire Protection Engineering: Cone Calorimeter." Massachusetts: Worcester Polytechnic Institute, 2006. Accessed: 13 March 2007. Available: <http://www.wpi.edu/Academics/Depts/Fire/Lab/Cone/>

Appendix A

Outer Layer

The outer shell is the first line of defense for a firefighter. It must provide protection against direct heat and flame as well as be durable. Some characteristics looked for in the outer layer are high thermal resistance, water absorption resistance, and cut and tear resistance. The main characteristics to look at when deciding on a thermal layer are its Thermal Stability, or temperature at which it loses its physical integrity, and its durability (Globe, 2006). Table 8 shows a comparison chart of different outer shell fabrics developed by Globe Manufacturers.

OUTER SHELL	Attribute										
	Durability	Cut Resistance	Tear Resistance	Fabric Strength	UV Resistance	Water Resistance	Formald, Off Gassing	Thermal Damage Tolerance	Thermal Protection	Heat Transfer Resistance	Cost
NOMEX® IIIA 7.5 osy (Many Colors)	High	Good	Good	Good	High	Good	Low	Low	Good	Good	\$
ADVANCE®/	High	High	Good	Good	Good	High	Low	Good	Very Good	Good	\$\$
BASOFIL®/ KEVLAR®	Low	High	Good	Good	Good	Good	High	Good	Very Good	Good	\$\$
Pbi®/KEVLAR®	High	High	Good	Good	Good	High	Low	High	Good	Good	\$\$\$
Pbi® with Matrix Technology	High	High	High	High	Very Good	High	Low	High	Good	Good	\$\$\$
MILLENNIA®	High	High	High	High	Good	High	Low	High	Low	Low	\$\$\$

Table 8: Globe Outer Shell Materials

The following are brief descriptions of the types of layers used for outer layers.

Nomex® IIIA

Nomex® IIIA has been around for nearly three decades. It is comprised of 93% Nomex®, 5% Kevlar® blend and 2% anti-static material. Nomex® IIIA is very durable as well as being very cost-effective which makes it the longest running outer shell used. One weakness it has is its susceptibility to degradation at temperatures exceeding 370°C. (Globe, 2006)

Advance®

Advance® builds on the dependability of Nomex® and adds more material endurance and strength by reinforcing with a Kevlar® blend (40% Nomex® and 60% Kevlar® blend). With this reinforcement it can withstand temperatures up to 566°C before showing signs of degradation. Advance® is also one of the lighter fabrics used for the outer shell. (Globe, 2006)

Basofil®

Basofil® is a newer outer shell fabric. Comprised of 40% Melamine and 60% Kevlar it yields high TPP values. With this superior protection comes a downside with the heavier weight of the fabric. Being relatively new on the market its durability has not been proven. (Globe, 2006)

Pbi®

Pbi® has performed exceptionally well in all service categories. Pbi® is comprised of 40% Polybenzimidazole and 60% Kevlar® blend. It is designed to withstand temperatures up to 704°C, be very durable and retain flexibility. One important downside to this fabric is its lack of warning. Unlike other fabrics Pbi® does not change color from UV, so there is no warning of when it is losing tensile strength. (Globe, 2006)

Millenia®

Millenia® is another new fabric used for the outer shell layer. As with the Basofil® fabric, the durability of this fabric is still unknown due to lack of field data. It is proven to have excellent tensile and tear strength as well as the best results in the

abrasion resistance test. Millenia® can be safely used around temperatures in excess of 704°C without any performance drops. (Globe, 2006)

Moisture Barrier

A moisture barrier functions as a sponge; it absorbs moisture yet allows it to evaporate. The Globe Manufacturing Company develops and produces several types of firefighter suits. Globe is the largest manufacturer of structural fire suits and developed three moisture textile technologies called microporous, monolithic, and bi-component textiles. (Globe, 2006)

Microporous Textiles

The microporous textile can either be designed to absorb water or repel water or anything in between. This textile functions by allowing small openings to pass air or water through and is usually based of PolyTetraFlouroEthylene (PTFE) or polyurethane. (Globe, 2006)

Monolithic Textiles

Little or no passage of air is permitted through monolithic textiles. The current monolithic textile technologies are coated with water repellents. These water repellent coatings are based of neoprene, whereas few somewhat breathable coatings include bases of polyurethane and polyester. (Globe, 2006)

Bi-component Textiles

Bi-component textiles are referred to as textiles that combine the monolithic and microporous technologies to create a unique textile. Some creations of bi-component textiles include Polyurethane/PTFE blends and polyurethane blends. The Crosstech® is comprised of a microporous and hydrophobic (water resistant) blend made of PTFE. This moisture barrier can be laundered and reused and still withstand 260°C for five minutes.

The RT7100® is another bi-component textile and a PTFE technology that is “laminated to NOMEX® non-woven substrate.” The Stedair® is a monolithic and microporous blend that is not only thermal and hydrostatic resistant but also tear resistant. This product is a PTFE technology that also protects against certain chemicals. (Globe) Table 9 compares several Globe moisture barriers.

FILM SUBSTRATE	ATTRIBUTE				
	Total Heat Loss	Thermal Insulation	Substrate Durability	Film Durability	Cost
CROSSTECH® NOMEX® Woven (GLOBE #4)	High	Moderate	High	High	\$\$\$
RT7100® DUPONT Nonwoven (Globe D)	Moderate	High	Moderate	Moderate	\$\$
STEDAIR 3000® NOMEX® E-89™ (Globe E)	High	Moderate	Moderate	High	\$\$
COMFORT ZONE® BASOFIL® Nonwoven (Globe C)	Low	High	Low	Moderate	\$

Table 9: Comparison of Globe Moisture Barriers

Thermal Liner

The thermal liner is the innermost layer and provides about 73% of the thermal protection of fire suits. Globe Manufacturing Company found that thermal liners function best when it is thin and light-weight. Thermal liners are marketed to serve different purposes. For example, the Caldura® SL Platinum is lightweight and built with NOMEX® filament/spun face cloth that is “designed to facilitate movement donning/doffing and minimize fatigue while still maintaining good wickability.” (Globe, 2006)

The Caldura® Platinum has the same fabrication as the Caldura® SL Platinum but provides better thermal protection performance (TPP) and is heavier. A much lighter thermal liner is the Aralite® Quilt Liner which is composed of recycled KEVLAR®

fibers as well as new fibers. Drawbacks of this textile's design include the high stress areas will ultimately wear out. (Globe, 2006)

The 2-layer NOMEX®E-89™ is not only lightweight but also has high total heat loss values. The lightweight characteristics are due to woven aramid fibers that, in effect, provide excellent mobility. A drawback to this textile is that Globe Manufacturing Company is the only company that manufactures this material. (Globe, 2006)

One of the longest lasting designs on the market, the Q-9®, is constructed from re-processed NOMEX® quilted aramid batt. This thermal liner is one of the heaviest and also has reduced breathability. (Globe, 2006)

Appendix B

Testing Procedure for Firefighter Protective Clothing

- 1) Record Test Information:
 - a) Date/Time
 - b) List Objectives of Today's Test
 - c) Team Data:
 - i) Supervisor
 - ii) Operator
 - iii) Safety
 - iv) Igniter
 - v) Data Collector
 - vi) Visitors
 - d) Weather Conditions
 - i) General
 - ii) Temperature
 - iii) Wind (Speed/Direction)
 - e) MSA Ultima gas sensor value (Should be zero)
- 2) General Procedures Prior to Testing:
 - a) Inspect around Burn Compartment for any combustible materials
 - i) Remove any found
 - b) Inspect Gypsum Wall Board and KaoWool for any failures
 - c) Sweep and mop area around room
 - d) Check all equipment to ensure proper function
 - i) Radios
 - ii) Garden Hose
 - iii) Personal Protective Equipment
 - iv) Computer/Multiplexer
 - v) Flow Controller Computer
 - vi) Vaporizer
 - (1) Turn on Briefly to verify operation
 - vii) Video Equipment
 - viii) Manikin Track
 - ix) Manikin Clothing (appropriately fitting, secure, no bare manikin showing)
 - e) Check and record Ultima gas sensor value (if not already done)
 - f) Perform Leak Check on Propane delivery system with 100 psi Nitrogen
 - i) SEE WOODWARD THESIS FOR PROPER PROCEDURE
 - g) Lay and Charge Fire Suppression Hose
 - h) Call ADT at (888) 831 – 5967
 - i) Give the following Data
 - (1) System Phone Number: (508) 831 – 5967
 - (2) System to be placed in test mode until ____ (Record Time)
 - i) Open Garage Doors on North and West side of Building and raise blue tarp cordoning building sections

- j) Check that trap is closed
- k) Charge Propane Delivery System
 - i) Open Propane Tank Slowly
 - ii) Check for leaks
 - iii) Open valves on remaining propane tanks
 - iv) Allow the tanks to equalize
 - v) Open Valve B
 - vi) Record Pressure at Manifold
- l) Wait until vaporizer has reached 60°C
- 3) Ignition:
 - a) Open Valve C
 - b) Ignite cardboard with propane torch and place on one burners
 - i) Evacuate burn room
 - c) Operator: Open ignition valve for each burner with burning cardboard on it
 - i) If cardboard extinguishes prior to gas ignition:
 - (1) Turn off gas to that burner
 - (2) Wait until remaining burners with cardboard ignite
 - (3) Enter, reignite cardboard
 - (4) Evacuate room
 - (5) Operator: Turn on ignition valve for burner.
 - d) After all ignition burners are operating, Operator: Turn on ignition on remaining burners (without cardboard)
 - e) Wait until all burners have ignited
- 4) Test Method for Standard Firefighter Protective Clothing:
 - a) Position clothed manikin 3+ meters from burners (outside room)
 - b) Place thermal shield between manikin and burners while fire grows to set size.
 - c) Set the flow controller to specified HRR rate (1.5 MW)
 - d) Begin gathering test data: Start Labview VI.
 - e) Allow fire to “level off” to constant for 30 seconds.
 - f) Remove thermal shield and start manikin moving through flames at predetermined speed settings:
 - i) .8 m/s (5 Turns)
 - ii) .64 m/s (4 Turns)
 - iii) .48 m/s (3 Turns)
 - iv) .32 m/s (2 Turns)
 - v) .16 m/s (1 Turn from 0)
 - g) After manikin has exited the back side of the room and is now 3+ meters from burners, reduces flow meter back to ignition setting.
 - h) Turn off TEST valves
 - i) After ~10 seconds, stop data gathering
 - j) Turn fan on clothed manikin
 - k) After clothing has sufficiently cooled, remove clothing.
 - l) Keep fan on bare manikin.
 - m) After sensors have dropped back to below ~25°C (or to ~ambient) manikin is ready to be tested again.
- 5) Post Test:

- a) Shut down propane delivery system:
 - i) Close valves at propane tanks
 - ii) Allow fires to burn remaining propane in system and decrease in size
 - iii) Open all TEST valves
 - iv) Open Nitrogen
 - v) Set Nitrogen regulator to 5 PSI
 - vi) Open valves A1, A2, A3, A4
 - vii) Allow lines to completely purge of propane (see bluish flames before burnout)
 - viii) Once flames are out, close nitrogen tank
 - ix) Close all control valves
 - x) Close all valves: (C, B, A1, A2, A3, A4)
- b) Turn off Vaporizer
- c) Open side doors to test room to allow it to cool
 - i) Wait until you can hold your hand to the gypsum board in the room
- d) Shut down the exhaust system
- e) Discharging and coil garden hose
- f) With AFFF foam, spray all edges of room, corners, and all signs of gypsum burning.
- g) Check the top of the compartment for any smoldering fires
- h) Close warehouse garage doors
- i) Personnel must remain at test site for 1 hr after test is completed
- j) Close test Room Doors
- k) If before time ADT is turning system back on, Call ADT and ask for system to be put back online.
- l) Close and lock propane storage shed
- m) Close and lock warehouse exit doors